Order Number 8918601

A fully two-dimensional flux-corrected transport algorithm for hyperbolic partial differential equations

Huang, Sen-Wei, Ph.D.

University of Alaska Fairbanks, 1989

U·M·I
300 N. Zeeb Rd.
Ann Arbor, MI 48106

A FULLY TWO–DIMENSIONAL FLUX–CORRECTED TRANSPORT ALGORITHM FOR HYPERBOLIC PARTIAL DIFFERENTIAL EQUATIONS

A

Thesis

Presented to the Faculty of the
University of Alaska in Partial Fulfillment
of the Requirements
for the Degree of

DOCTOR OF PHILOSOPHY

By
Sen–Wei Huang, M.S.
Fairbanks, Alaska
May 1989

A FULLY TWO-DIMENSIONAL FLUX-CORRECTED TRANSPORT ALGORITHM FOR HYPERBOLIC PARTIAL DIFFERENTIAL EQUATIONS

By

Sen-Wei Huang

RECOMMENDED:

Walter Tape

J. P. Lambert

Jon E. Lee

Clif Funderburk

Mary A. Gislason
Chairman, Advisory Committee

Clif Funderburk
Department Head

APPROVED:

Clif Funderburk, Acting
Dean, College of Liberal Arts

Dean of the Graduate School

4/24/89
Date

Abstract

Numerical solutions of the hyperbolic partial differential equation, $\frac{\partial \rho}{\partial t}+\vec{\nabla}\cdot(\rho\vec{u}) = 0$, will generally encounter the difficulties of large diffusion and oscillations near steep gradients or discontinuities. The method of Flux–Corrected Transport (FCT) developed by Boris and Book has conquered these difficulties for the one–dimensional case. Motivated by this one–dimensional FCT algorithm, a fully two–dimensional FCT algorithm is developed in this present work. This fully two–dimensional FCT algorithm is a two–step procedure: (1) the transport scheme, and (2) the antidiffusion scheme. The second step of the procedure could also be replaced by an application of the one–dimensional antidiffusion algorithm in the x direction and the y direction separately. The stability, phase shift errors and positivity for the fully two–dimensional transport scheme are analyzed. Test results are presented. The possibility of the extension of the FCT method to three dimensions are discussed.

Table of Contents

List of Figures

Acknowledgments

I would like to thank all of my committee members, Dr. Gary Gislason, Dr. J. Patrick Lambert, Dr. Clifton Lando, Dr. Lou–Chuang Lee and Dr. Walter Tape, who generously contributed their time in reviewing my thesis and giving their helpful suggestions which enabled me to complete this thesis.

I also wish to express my sincere appreciation to my thesis advisor, Dr. Gary Gislason, who suggested the topic of this thesis and assisted me throughout my work and study here. Without his guidance, encouragement and recommendation, I do not believe I could have completed my thesis and studies so smoothly.

Thanks also go to all of the faculty and the secretaries in Department of Mathematical Sciences. Without their help and support, it would have been impossible for me to complete my studies here.

SECTION 1:

Introduction

Consider the initial value problem consisting of the following hyperbolic partial differential equation and initial condition,

$$\frac{\partial \rho}{\partial t} + \vec{\nabla} \cdot (\rho \vec{u}) = 0 \tag{1.1}$$

$$\rho = \rho(\vec{r}, 0)$$

where ρ represents generalized density or the transported quantity, $\vec{r}$ is the position vector, and $\vec{u}$ is velocity.

In the one–dimensional constant velocity case most of the finite difference methods of second–order schemes, such as Lax–Wendroff and leapfrog [15], will approximate the solutions fairly well in a region where the density, ρ, is smooth. Those higher order (order 2 or above) schemes, however, will suffer from Gibbs–type oscillations in ρ, particularly near steep gradients in ρ. Lower order schemes, such as donor cell and Lax–Friedrichs, will produce no oscillations but suffer from excessive numerical diffusion. To compute the shocks or the steep–gradient solutions to equation (1.1), a technique called Flux–Corrected Transport (FCT) was developed by Boris and Book [1,2,3,4,5,6] which embodies the best of both of concepts. The FCT algorithm consists of three finite difference operations: 1) transport, 2) diffusion, and 3) antidiffusion. In [3], the transport and diffusion are performed as a single operation. A square–wave test case has shown that the one–dimensional FCT algorithm produces a solution without overshoots or undershoots, but with residual fourth–order diffusion which rounds the corners of the square wave somewhat. This one–dimensional FCT algorithm is described briefly in Section 2.

To extend the FCT technique to the two–dimensional case, a fully two–dimensional transport algorithm is developed in Section 3, which is based on the motivating principles set forth in [3]. This fully two–dimensional transport algorithm convects the fluid–elements in concert on the x–y plane, which preserves the positivity and conserves the mass, but has a strong diffusion in the transported densities $\{\rho^{TD}\}$. In Section 4 the stability and positivity of this fully two–dimensional transport algorithm are analyzed for a constant velocity field. Following this fully two–dimensional transport algorithm, two antidiffusion algorithms are developed in Section 5. Firstly, a fully two–dimensional antidiffusion algorithm is shown in Section 5.1, in which the flux limiter for this fully two–dimensional antidiffusion algorithm is defined in the spirit of Zalesak's work [24]. Secondly, a straightforward application of the one–dimensional antidiffusion algorithm [3] to each coordinate separately is shown in Section 5.2. In Section 6, two numerical examples are shown to exhibit how well our fully two–dimensional FCT algorithms work in handling the shock problems. The comparsion of Lax–Wendroff scheme with this FCT algorithm is also shown in this section. Finally, the possibility of extending the FCT technique to three dimensions is investigated in Section 7.

This fully two–dimensional FCT algorithm can be used to solve the fluid equations which satisfy (1.1), such as the following system of equations for an ideal inviscid fluid,

$$\frac{\partial \rho}{\partial t} + \vec{\nabla} \cdot (\rho \vec{v}) = 0$$

$$\frac{\partial}{\partial t}(\rho \vec{v}) + \vec{\nabla} \cdot (\rho \vec{v} \vec{v}) = -\nabla \rho$$

$$\frac{\partial}{\partial t}(\rho E) + \vec{\nabla} \cdot [(P + \rho E)\vec{v}] = 0$$

where ρ, $\vec{v}$, P and E are the fluid density, velocity, pressure and specific energy, respectively. These equations can be solved for the two–dimensional case by using this FCT algorithm. In addition, the equations for the conservation of mass, momentum and energy, the equations for ion flow in electric and magnetic fields, and the equations for molecular flow, etc., can

be solved by this algorithm. The FCT algorithm, which handles well the steep gradients in ρ, may be a time–consuming and expensive algorithm in other cases. Unless the density, ρ, has steep gradients, the usual schemes, such as Lax–Wendroff, should be used instead of the FCT algorithm.

SECTION 2:

One–Dimensional Flux–Corrected Transport

The hyperbolic partial differential equation of (1.1) in one dimension is

$$\frac{\partial \rho}{\partial t} + \frac{\partial}{\partial x}(\rho u) = 0, \tag{2.1}$$

where the density ρ is convected with velocity u. We describe briefly the one–dimensional FCT algorithm as it appears in [3].

2.1 Transport Stage

Let $\rho_i^n = \rho(x_i, t_n)$ be the density at $x_i = i\Delta x$ and $t_n = n\Delta t$ and u_i the velocity at $x_i = i\Delta x$. The geometric interpretation of one–dimensional FCT transport is shown in Figure 1. Linear interpolations are used throughout so that the mass is conserved and the transported densities $\{\rho_i^{TD}\}$ are nonnegative as long as $|u\frac{\Delta t}{\Delta x}| < \frac{1}{2}$ and $\{\rho_i^n\}$ are nonnegative.

At the end of transport, the fluid–element has been converted and deformed as shown in Figure 1(b). The heights of the sides of the trapezoid, ρ_i^T and ρ_{i+1}^T in Figure 1(b), are given by

$$\rho_i^T = \rho_i^n \frac{\Delta x}{\Delta x + \Delta t(u_{i+1} - u_i)} \quad \text{and} \quad \rho_{i+1}^T = \rho_{i+1}^n \frac{\Delta x}{\Delta x + \Delta t(u_{i+1} - u_i)}. \tag{2.2}$$

It is clear from these given heights in (2.2) that the area of the trapezoid, hence the mass, is fully conserved. It is also clear that the values ρ_i^T and ρ_{i+1}^T are always nonnegative if all of the $\{\rho_i^n\}$ are nonnegative and $|u\frac{\Delta t}{\Delta x}| < \frac{1}{2}$. We treat all of the fluid–elements in the same way and independently. Define $\{\rho_i^{TD}\}$ to be the interpolation of the displaced

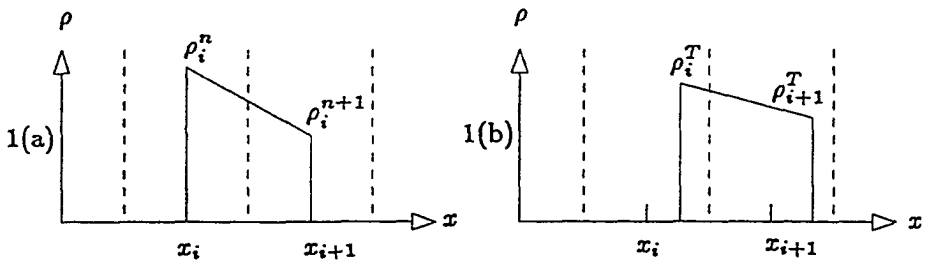

Fig. 1 The transport of a fluid–element in the one–dimensional case. Figure 1(a) is the fluid–element before transport at time $t = n\Delta t$. Figure 1(b) is the fluid–element after transport at time $t = (n+1)\Delta t$. Both are interpolated by a straight line.

fluid–elements onto the original grid points $\{x_i\}$. Let ρ_i^{TD} be given by the division of the sum of two adjacent areas over the interval $(x_i - \frac{1}{2}\Delta x \leq x \leq x_i + \frac{1}{2}\Delta x)$ of width Δx. The complete transport algorithm which relates the transported and diffused density $\{\rho_i^{TD}\}$ to $\{\rho_i^n\}$ is

$$\rho_i^{TD} = \frac{1}{2}Q_-^2(\rho_{i-1}^n - \rho_i^n) + \frac{1}{2}Q_+^2(\rho_{i+1}^n - \rho_i^n) + (Q_+ + Q_-)\rho_i^n, \tag{2.3}$$

where

$$Q_\pm = \frac{\frac{1}{2} \mp u_i \frac{\Delta t}{\Delta x}}{1 \pm (u_{i\pm1} - u_i)\frac{\Delta t}{\Delta x}}.$$

For a uniform velocity field, letting $\epsilon = u\frac{\Delta t}{\Delta x}$, equation (2.3) reduces to a simple form

$$\rho_i^{TD} = \rho_i^n - \frac{\epsilon}{2}(\rho_{i+1}^n - \rho_{i-1}^n) + (\frac{1}{8} + \frac{\epsilon^2}{2})(\rho_{i+1}^n - 2\rho_i^n + \rho_{i-1}^n). \tag{2.4}$$

In the zero velocity case, the transport equation (2.4) produces a strong net diffusion

$$\rho_i^{TD} = \rho_i^n + \frac{1}{8}(\rho_{i+1}^n - 2\rho_i^n + \rho_{i-1}^n). \tag{2.5}$$

However, this strong diffusion is the basis of FCT which ensures the positivity of the density ρ during transport.

2.2 Antidiffusive Stage

The antidiffusive stage of FCT attempts to remove numerical diffusion introduced in the transport stage. The means for removal of an equal and opposite net diffusion suggested by (2.5) would be given by

$$\begin{aligned}\rho_i^{n+1} &= \rho_i^{TD} - \frac{1}{8}(\rho_{i+1}^{TD} - 2\rho_i^{TD} + \rho_{i-1}^{TD}) \\ &= \rho_i^{TD} - \frac{1}{8}(\rho_{i+1}^{TD} - \rho_i^{TD}) + \frac{1}{8}(\rho_i^{TD} - \rho_{i-1}^{TD}).\end{aligned} \tag{2.6}$$

But, this produces physically unreasonable minima and maxima in ρ. A corrected antidiffusive flux has been introduced in [3] as

$$f_{i+\frac{1}{2}}^c = s \cdot \max[0, \min(s \cdot f_{i-\frac{1}{2}}, \text{“}\tfrac{1}{8}\text{”}|f_{i+\frac{1}{2}}|, s \cdot f_{i+\frac{3}{2}})], \tag{2.7}$$

where

$$f_{i+\frac{1}{2}} = \rho_{i+1}^{TD} - \rho_i^{TD}$$

$$s = \text{sign}\{f_{i+\frac{1}{2}}\}.$$

This corrected antidiffusive flux $\{f_{i+\frac{1}{2}}^c\}$ will remove the diffusion introduced in (2.3) and produce no physically unreasonable minima or maxima by letting

$$\rho_i^{n+1} = \rho_i^{TD} - f_{i+\frac{1}{2}}^c + f_{i-\frac{1}{2}}^c. \tag{2.8}$$

The “$\frac{1}{8}$” in (2.7) is the adjustable coefficient which is given in [3]. Let $\overline{\rho} = \sqrt{\rho_{max}\rho_{min}}$. Then

$$\text{“}\tfrac{1}{8}\text{”} = \begin{cases} \frac{1}{8}[1 + (1 - \frac{0.25\overline{\rho}}{|f_{i+\frac{1}{2}}|})^2], & \text{if} \quad f_{i+\frac{1}{2}} \geq 0.25\overline{\rho}. \\ \frac{1}{8}, & \text{otherwise.} \end{cases} \tag{2.9}$$

A square–wave test case is shown in Figure 2. The square–wave has almost been preserved during transport and produces no overshoot or undershoot at shocks.

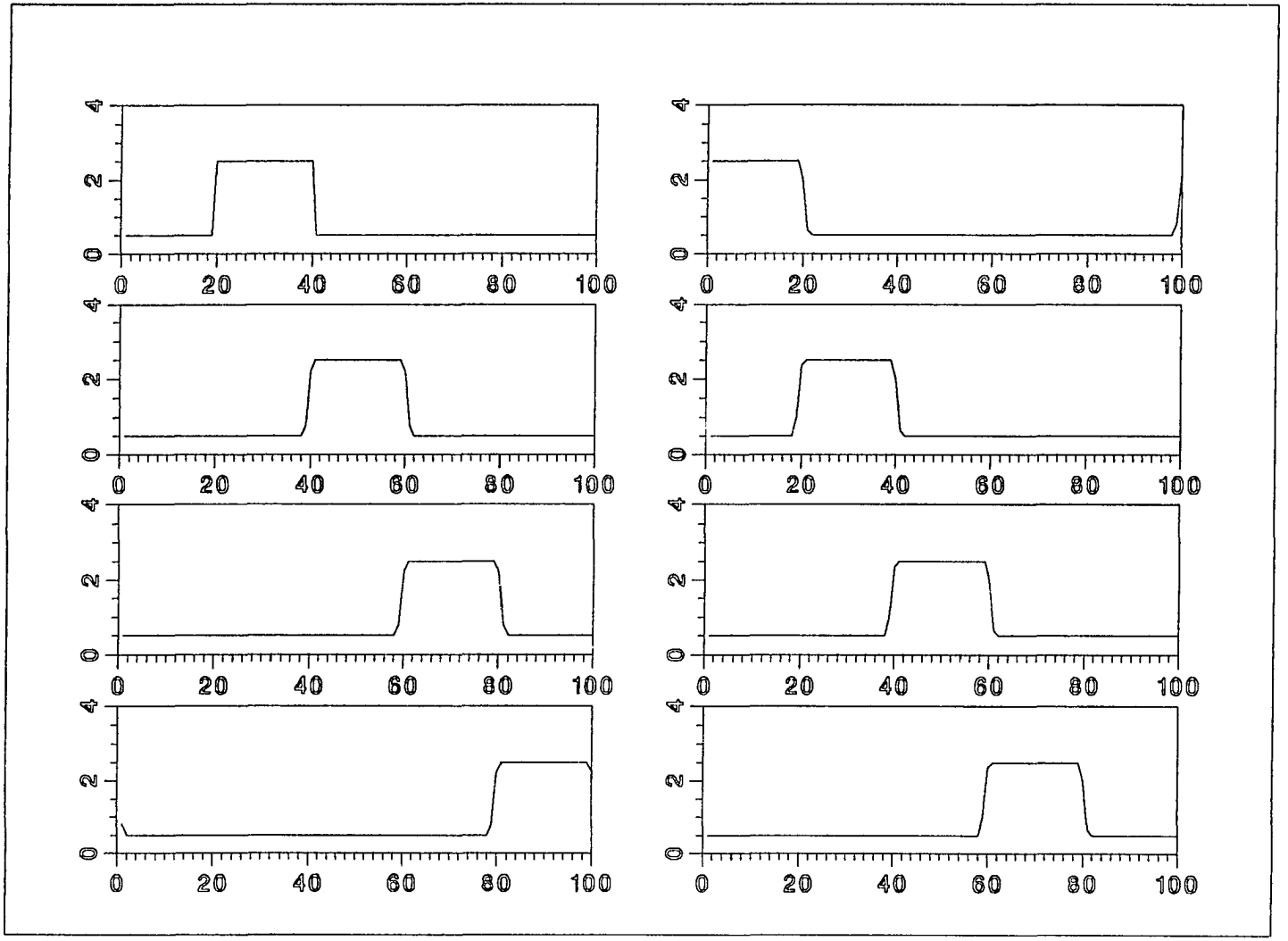

Fig. 2 Square-wave test for the one-dimensional FCT algorithm. With $\Delta x = 1$, $\Delta t = 0.2$, velocity $u = 1$ and periodic boundaries, data are ploted every 100 cycles in this test problem.

SECTION 3:

The Fully Two–Dimensional Transport Scheme

Consider the two–dimensional hyperbolic equation of (1.1),

$$\frac{\partial \rho}{\partial t} + \frac{\partial}{\partial x}(\rho v) + \frac{\partial}{\partial y}(\rho w) = 0, \tag{3.1}$$

where the density ρ is convected by the velocity $\vec{u} = < v, w >$.

In Cartesian coordinates, let Δt be the equal time advancement for each cycle and let Δx and Δy be the uniform spacing of the gridwork in the x and in y directions respectively; We denote the density ρ at $x = x_i$,$y = y_j$ and $t = t_n$ as $\rho(x_i, y_j, t_n) = \rho^n_{i,j}$, where $x_i = i\Delta x$, $y_j = j\Delta y$ and $t_n = n\Delta t$.

Our fully two–dimensional transport algorithm proceeds by considering individually each fluid–element on the rectangular region

$$R_{i+\frac{1}{2},j+\frac{1}{2}} = \{ (x, y) \mid \quad x_i \leq x \leq x_{i+1} \, , \, y_j \leq y \leq y_{j+1} \}. \tag{3.2}$$

The density surface over $R_{i+\frac{1}{2},j+\frac{1}{2}}$ is interpolated by the determinant

$$\begin{vmatrix} 1 & x & y & xy & Z \\ 1 & x_i & y_j & x_i y_j & \rho^n_{i,j} \\ 1 & x_{i+1} & y_j & x_{i+1} y_j & \rho^n_{i+1,j} \\ 1 & x_{i+1} & y_{j+1} & x_{i+1} y_{j+1} & \rho^n_{i+1,j+1} \\ 1 & x_i & y_{j+1} & x_i y_{j+1} & \rho^n_{i,j+1} \end{vmatrix} = 0. \tag{3.3}$$

which can be reduced to an equation of the form

$$Z(x, y) = A + Bx + Cy + Dxy. \tag{3.4}$$

The volume of this fluid–element interpolated by (3.4) over the region $R_{i+\frac{1}{2},j+\frac{1}{2}}$ is given as

$$V_{i+\frac{1}{2},j+\frac{1}{2}} = \int\int \quad Z(x, y) \quad dR_{i+\frac{1}{2},j+\frac{1}{2}} \, . \tag{3.5}$$

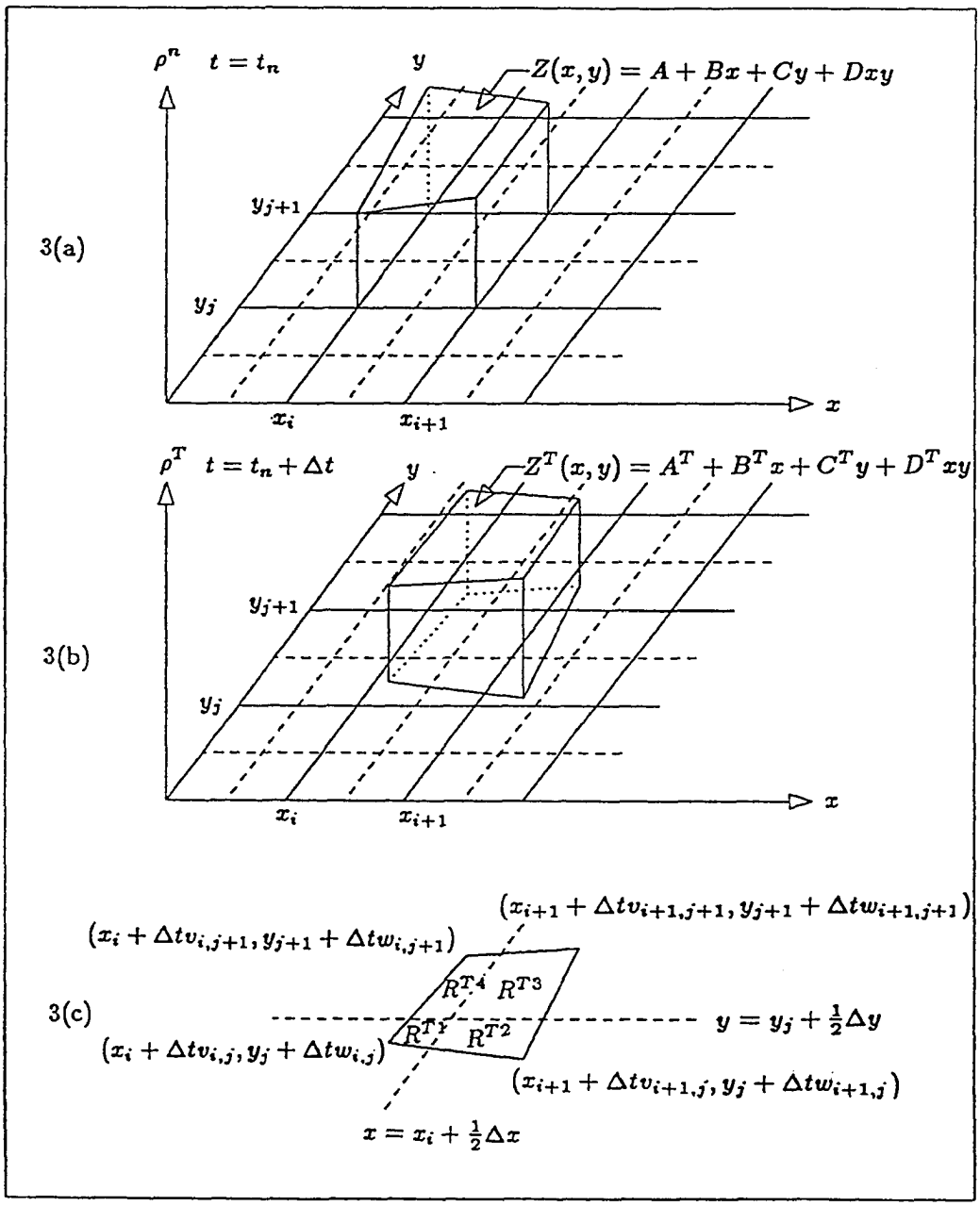

Fig. 3 Transport of the fluid–element in the two–dimensional case. Figure 3(a) indicates the location and interpolation of fluid–element before transport. Figure 3(b) indicates the fluid–element after transport. Figure 3(c) indicates the region of the transported fluid–element in the $x - y$ plane, where $R^T_{i+\frac{1}{2},j+\frac{1}{2}}$ is the union of $R^{T1}_{i+\frac{1}{2},j+\frac{1}{2}}$, $R^{T2}_{i+\frac{1}{2},j+\frac{1}{2}}$, $R^{T3}_{i+\frac{1}{2},j+\frac{1}{2}}$ and $R^{T4}_{i+\frac{1}{2},j+\frac{1}{2}}$.

Figure 3 shows the geometric interpretation of the fluid transport during one time step. Before the transport, when $t = t_n$, the fluid–element is on the region $R_{i+\frac{1}{2},j+\frac{1}{2}}$ as shown in Figure 3(a). At the end of the cycle, when $t = t_n + \Delta t$, the fluid–element has been convected and deformed as shown in Figure 3(b). The movement of four densities and grid points on $R_{i+\frac{1}{2},j+\frac{1}{2}}$, after one cycle, is given as

$$\begin{aligned}
(x_i, y_j, \rho^n_{i,j}) &\longmapsto (x^T_{i,j}, y^T_{i,j}, \rho^T_{i,j}) \\
(x_{i+1}, y_j, \rho^n_{i+1,j}) &\longmapsto (x^T_{i+1,j}, y^T_{i+1,j}, \rho^T_{i+1,j}) \\
(x_{i+1}, y_{j+1}, \rho^n_{i+1,j+1}) &\longmapsto (x^T_{i+1,j+1}, y^T_{i+1,j+1}, \rho^T_{i+1,j+1}) \\
(x_i, y_{j+1}, \rho^n_{i,j+1}) &\longmapsto (x^T_{i,j+1}, y^T_{i,j+1}, \rho^T_{i,j+1}),
\end{aligned}$$

where

$$\begin{aligned}
(x^T_{i,j}, y^T_{i,j}, \rho^T_{i,j}) &= (x_i + \Delta t v_{i,j}, y_j + \Delta t w_{i,j}, \rho^T_{i,j}) \\
(x^T_{i+1,j}, y^T_{i+1,j}, \rho^T_{i+1,j}) &= (x_{i+1} + \Delta t v_{i+1,j}, y_j + \Delta t w_{i+1,j}, \rho^T_{i+1,j}) \\
(x^T_{i+1,j+1}, y^T_{i+1,j+1}, \rho^T_{i+1,j+1}) &= (x_{i+1} + \Delta t v_{i+1,j+1}, y_{j+1} + \Delta t w_{i+1,j+1}, \rho^T_{i+1,j+1}) \\
(x^T_{i,j+1}, y^T_{i,j+1}, \rho^T_{i,j+1}) &= (x_i + \Delta t v_{i,j+1}, y_{j+1} + \Delta t w_{i,j+1}, \rho^T_{i,j+1}).
\end{aligned}$$

In the analysis of this paper we consider only the case when $|v\frac{\Delta t}{\Delta x}| < \frac{1}{2}$ and $|w\frac{\Delta t}{\Delta y}| < \frac{1}{2}$ so that no grid point can convect past the cell boundaries in a cycle, as indicated by dashed lines in Figure 3(a). This restriction is a sufficient condition for stability in our transport algorithm. Let

$$\begin{aligned}
R^T_{i+\frac{1}{2},j+\frac{1}{2}} = \{ &\text{ the region enclosed by the quadrilateral having the four vertices,} \\
&(x^T_{i,j}, y^T_{i,j}), (x^T_{i+1,j}, y^T_{i+1,j}), (x^T_{i+1,j+1}, y^T_{i+1,j+1}) \text{and} (x^T_{i,j+1}, y^T_{i,j+1})\}
\end{aligned} \tag{3.6}$$

and let $R^{T1}_{i+\frac{1}{2},j+\frac{1}{2}}$, $R^{T2}_{i+\frac{1}{2},j+\frac{1}{2}}$, $R^{T3}_{i+\frac{1}{2},j+\frac{1}{2}}$ and $R^{T4}_{i+\frac{1}{2},j+\frac{1}{2}}$ be the four subregions of $R^T_{i+\frac{1}{2},j+\frac{1}{2}}$, as shown in Figure 3(c), which are formed when $R^T_{i+\frac{1}{2},j+\frac{1}{2}}$ is divided by two perpendicular

lines $x = x_i + \frac{1}{2}\Delta x$ and $y = y_j + \frac{1}{2}\Delta y$. The densities ρ on the transported area $R^T_{i+\frac{1}{2},j+\frac{1}{2}}$ are interpolated by equation

$$\begin{vmatrix} 1 & x & y & xy & Z^T \\ 1 & x^T_{i,j} & y^T_{i,j} & (x^T_{i,j})(y^T_{i,j}) & \rho^T_{i,j} \\ 1 & x^T_{i+1,j} & y^T_{i+1,j} & (x^T_{i+1,j})(y^T_{i+1,j}) & \rho^T_{i+1,j} \\ 1 & x^T_{i+1,j+1} & y^T_{i+1,j+1} & (x^T_{i+1,j+1})(y^T_{i+1,j+1}) & \rho^T_{i+1,j+1} \\ 1 & x^T_{i,j+1} & y^T_{i,j+1} & (x^T_{i,j+1})(y^T_{i,j+1}) & \rho^T_{i,j+1} \end{vmatrix} = 0. \tag{3.7}$$

which can be reduced to the equation

$$Z^T(x,y) = A^T + B^T x + C^T y + D^T xy\,. \tag{3.8}$$

The corresponding volume of the transported fluid–element, interpolated by $Z^T(x,y)$, over the region $R^T_{i+\frac{1}{2},j+\frac{1}{2}}$ is given by

$$V^T_{i+\frac{1}{2},j+\frac{1}{2}} = \iint \quad Z^T(x,y) \quad dR^T_{i+\frac{1}{2},j+\frac{1}{2}}\,. \tag{3.9}$$

Also, the volumes of the four fluid subelements over the subregions, $R^{TI}_{i+\frac{1}{2},j+\frac{1}{2}}$, I = 1, 2, 3 and 4, and under the surface in (3.7) are given by

$$V^{TI}_{i+\frac{1}{2},j+\frac{1}{2}} = \iint \quad Z^T(x,y) \quad dR^{TI}_{i+\frac{1}{2},j+\frac{1}{2}} \quad , \quad I = 1,2,3,4\,. \tag{3.10}$$

In order to meet the requirement of the conservation of mass, the determination of the densities, $\rho^T_{i,j}$, $\rho^T_{i+1,j}$, $\rho^T_{i+1,j+1}$ and $\rho^T_{i,j+1}$, should make the volume, $V^T_{i+\frac{1}{2},j+\frac{1}{2}}$, of the transported fluid–element equal to the volume, $V_{i+\frac{1}{2},j+\frac{1}{2}}$, of the corresponding fluid–element before transport. Thus, we define $\rho^T_{i,j}$, $\rho^T_{i+1,j}$, $\rho^T_{i+1,j+1}$ and $\rho^T_{i,j+1}$ by the following two steps.

(I) Interpolate the densities on the transported region, $R^T_{i+\frac{1}{2},j+\frac{1}{2}}$, by the determinant

$$\begin{vmatrix} 1 & x & y & xy & \overline{Z} \\ 1 & x^T_{i,j} & y^T_{i,j} & (x^T_{i,j})(y^T_{i,j}) & \rho^n_{i,j} \\ 1 & x^T_{i+1,j} & y^T_{i+1,j} & (x^T_{i+1,j})(y^T_{i+1,j}) & \rho^n_{i+1,j} \\ 1 & x^T_{i+1,j+1} & y^T_{i+1,j+1} & (x^T_{i+1,j+1})(y^T_{i+1,j+1}) & \rho^n_{i+1,j+1} \\ 1 & x^T_{i,j+1} & y^T_{i,j+1} & (x^T_{i,j+1})(y^T_{i,j+1}) & \rho^n_{i,j+1} \end{vmatrix} = 0. \tag{3.11}$$

which can be reduced to the equation

$$\overline{Z}(x,y) = \overline{A} + \overline{B}x + \overline{C}y + \overline{D}xy\,. \tag{3.12}$$

The corresponding volume of $\overline{Z}(x,y)$ over $R^T_{i+\frac{1}{2},j+\frac{1}{2}}$ is

$$\overline{V} = \int\int \quad \overline{Z}(x,y) \quad dR^T_{i+\frac{1}{2},j+\frac{1}{2}}\,. \tag{3.13}$$

(II) Let $\kappa = \frac{V_{i+\frac{1}{2},j+\frac{1}{2}}}{\overline{V}}$. (3.14)

If $\overline{V} \neq 0$, then define the transported densities to be

$$\begin{aligned} \rho^T_{i,j} &\equiv \kappa\rho^n_{i,j} \\ \rho^T_{i+1,j} &\equiv \kappa\rho^n_{i+1,j} \\ \rho^T_{i+1,j+1} &\equiv \kappa\rho^n_{i+1,j+1} \\ \rho^T_{i,j+1} &\equiv \kappa\rho^n_{i,j+1}\,. \end{aligned} \tag{3.15}$$

Otherwise let all of them be zero.

§ Theorem: $V^T_{i+\frac{1}{2},j+\frac{1}{2}} = V_{i+\frac{1}{2},j+\frac{1}{2}}$ (3.16)

Proof: Substitute (3.15) into (3.7) and then compare (3.7) with (3.11), we have the identity

$$Z^T(x,y) = \kappa\overline{Z}(x,y)$$

Thus,

$$\begin{aligned} V^T_{i+\frac{1}{2},j+\frac{1}{2}} &= \int\int \quad Z^T(x,y) \quad dR^T_{i+\frac{1}{2},j+\frac{1}{2}} \\ &= \int\int \quad \kappa\overline{Z}(x,y) \quad dR^T_{i+\frac{1}{2},j+\frac{1}{2}} \\ &= \kappa\cdot\overline{V} \\ &= V_{i+\frac{1}{2},j+\frac{1}{2}} \end{aligned}$$

It is clear from the above theorem, (3.16), that the volume of the fluid element, hence the densities or the mass, is fully conserved during transport. It is also clear from (3.15) that

the densities $\{\rho^T_{i,j}\}$ are always non–negative if all of the densities $\{\rho^n_{i,j}\}$ are non–negative before the transport.

Let the interpolation of the displaced fluid–element back onto the grid point (x_i, y_j) be $\rho^{TD}_{i,j}$, which is given simply by dividing the sum of all of the subvolumes over the region

$$R_{i,j} = \{\,(x,y)\,|\quad x_i - \frac{1}{2}\Delta x \le x \le x_i + \frac{1}{2}\Delta x\,,\, y_j - \frac{1}{2}\Delta y \le y \le y_j + \frac{1}{2}\Delta y\,\} \qquad (3.17)$$

by the area of $R_{i,j}$. Since the transport of the grid points is restricted by $|\frac{\Delta t}{\Delta x}v| < \frac{1}{2}$ and $|\frac{\Delta t}{\Delta y}w| < \frac{1}{2}$, no grid point can convect past the cell boundaries, hence the volumes of four subfluid–elements, $V^{TI}_{i+\frac{1}{2},j+\frac{1}{2}}$, I = 1, 2, 3 and 4, are always non–negative. This assures that the interpolation of the density, $\rho^{TD}_{i,j}$, back onto the grid point (x_i, y_j) is always non–negative.

§ Lemma: Let R={the region enclosed by the quadrilateral having the four vertices,

$$(x_1, y_1),\ (x_2, y_2),\ (x_3, y_3) \text{ and } (x_4, y_4)\ \}$$

then we have

$$\begin{aligned}
\int\int 1\,dR =& \frac{1}{2}[(x_1 - x_3)(y_2 - y_4) + (x_2 - x_4)(y_3 - y_1)] \\
\int\int x\,dR =& \frac{1}{6}[y_1(x_4^2 + x_4x_1 - x_1x_2 - x_2^2) + y_2(x_1^2 + x_1x_2 - x_2x_3 - x_3^2) \\
&+ y_3(x_2^2 + x_2x_3 - x_3x_4 - x_4^2) + y_4(x_3^2 + x_3x_4 - x_4x_1 - x_1^2)] \\
\int\int y\,dR =& \frac{1}{6}[x_1(-y_4^2 - y_4y_1 + y_1y_2 + y_2^2) + x_2(-y_1^2 - y_1y_2 + y_2y_3 + y_3^2) \\
&+ x_3(-y_2^2 - y_2y_3 + y_3y_4 + y_4^2) + x_4(-y_3^2 - y_3y_4 + y_4y_1 + y_1^2)] \\
\int\int xy\,dR =& \frac{1}{24}[x_1^2(-y_4^2 - 2y_4y_1 + 2y_1y_2 + y_2^2) + x_2^2(-y_1^2 - 2y_1y_2 + 2y_2y_3 + y_3^2) \\
&+ x_3^2(-y_2^2 - 2y_2y_3 + 2y_3y_4 + y_4^2) + x_4^2(-y_3^2 - 2y_3y_4 + 2y_4y_1 + y_1^2) \\
&+ 2x_1x_2(-y_1^2 + y_2^2) + 2x_2x_3(-y_2^2 + y_3^2) + 2x_3x_4(-y_3^2 + y_4^2) \\
&+ 2x_4x_1(-y_4^2 + y_1^2)]
\end{aligned}$$

Proof: See Appendix A.

With the help of the Lemma, the complete transport algorithm which relates $\{\rho_{i,j}^{TD}\}$ to $\{\rho_{i,j}^{n}\}$ in the uniform velocity field $\vec{u} =< v, w >$ is given as (see Appendix B)

$$\rho_{i,j}^{TD} = \frac{1}{64}\left\{ \begin{array}{ccc} (1+2\eta)^2(1-2\phi)^2 & 2(3-4\eta^2)(1-2\phi)^2 & (1-2\eta)^2(1-2\phi)^2 \\ 2(1+2\eta)^2(3-4\phi^2) & 4(3-4\eta^2)(3-4\phi^2) & 2(1-2\eta)^2(3-4\phi^2) \\ (1+2\eta)^2(1+2\phi)^2 & 2(3-4\eta^2)(1+2\phi)^2 & (1-2\eta)^2(1+2\phi)^2 \end{array} \right\} \rho_{i,j}^{n} \tag{3.18}$$

where $\eta \equiv \frac{\Delta t}{\Delta x} v$ and $\phi \equiv \frac{\Delta t}{\Delta y} w$.

When the velocity is zero, the transport algorithm produces a strong net diffusion given by

$$\rho_{i,j}^{TD} = \rho_{i,j}^{n} + \frac{1}{64}\left\{ \begin{array}{ccc} 1 & 6 & 1 \\ 6 & -28 & 6 \\ 1 & 6 & 1 \end{array} \right\} \rho_{i,j}^{n} \tag{3.19}$$

This strong net diffusion prevents the overshoots and undershoots and ensures the positivity of ρ during transport. It is the basis of FCT. In the following sections a means of removing this diffusion will be developed and an analysis of stability and positivity will be made.

SECTION 4:

Stability and Positivity

4.1 Stability

Using von Neumann's method in [15], the stability of transport schemes for the constant velocity field are analyzed as follows.

(I) In the one–dimensional case, the hyperbolic equation of (2.1) with constant velocity u can be rewritten as

$$\frac{\partial \rho}{\partial t} + u\frac{\partial \rho}{\partial x} = 0 \tag{4.1}$$

The analytic solution to (4.1) is

$$\rho(x,t) = \rho(x - ut, 0) \tag{4.2}$$

If the given initial density at grid point x_i $(= i\Delta x)$ is $\rho_i^o = e^{\iota k i \Delta x}$, where $\iota \equiv \sqrt{-1}$ and k is the wave number, then the analytic solution $\rho(x,t)$ at $x = x_i$ and $t = t_n$ is $\rho_i^n = e^{\iota k i \Delta x} e^{-\iota k u n \Delta t}$. Substitution of those analytic solutions into the transport formula (2.4) will give rise to an amplification coefficient for one time step as

$$\frac{\rho_i^{TD}}{\rho_i^n} = 1 - (\frac{1}{4} + \epsilon^2)(1 - \cos k\Delta x) - \iota\epsilon \sin k\Delta x \tag{4.3}$$

The corresponding magnitude of the amplification in (4.3) is

$$\left|\frac{\rho_i^{TD}}{\rho_i^n}\right|^2 = [1 - (\frac{1}{4} + \epsilon^2)(1 - \cos k\Delta x)]^2 + [\epsilon \sin k\Delta x]^2 \tag{4.4}$$

For $|\epsilon| < \frac{1}{2}$, the magnitude of the amplification factor in (4.4) is always less than 1. This means the numerical wave always decays in time, hence the transport formula (2.4) is stable.

(II) In the two–dimensional case, with the constant velocity $\vec{u} =< v, w >$, the hyperbolic equation (3.1) is equivalent to

$$\frac{\partial \rho}{\partial t} + v\frac{\partial \rho}{\partial x} + w\frac{\partial \rho}{\partial y} = 0 \tag{4.5}$$

The analytic solution to (4.5) is

$$\rho(x, y, t) = \rho(x - vt, y - wt, 0) \tag{4.6}$$

If the given initial density at $\vec{r}$ is $\rho^o = e^{\iota \vec{k}\cdot\vec{r}}$, where $\iota \equiv \sqrt{-1}$, $\vec{r} =< x, y >$ is the position vector and $\vec{k} =< k_1, k_2 >$ is the wave number, then the analytic solution at $x = x_i$, $y = y_j$ and $t = t_n$ is

$$\rho^n_{i,j} = e^{\iota(k_1 i\Delta x + k_2 j\Delta y)} e^{-\iota(k_1 vn\Delta t + k_2 wn\Delta t)} \tag{4.7}$$

Substitution of (4.7) into the fully two–dimensional transport formula (3.18) gives the amplification coefficient for one time step as (see Appendix C, (I))

$$\begin{aligned} \rho^{TD}_{i,j} =& [1 - (\frac{1}{4} + \eta^2)(1 - \cos k_1\Delta x) - \iota\eta \sin k_1\Delta x] \\ & \cdot [1 - (\frac{1}{4} + \phi^2)(1 - \cos k_2\Delta y) - \iota\phi \sin k_2\Delta y] \cdot \rho^n_{i,j} \end{aligned} \tag{4.8}$$

and also gives the amplification factor as

$$\begin{aligned} \left|\frac{\rho^{TD}_{i,j}}{\rho^n_{i,j}}\right|^2 =& \{[1 - (\frac{1}{4} + \eta^2)(1 - \cos k_1\Delta x)]^2 + [\eta \sin k_1\Delta x]^2\} \\ & \cdot \{[1 - (\frac{1}{4} + \phi^2)(1 - \cos k_2\Delta y)]^2 + [\phi \sin k_2\Delta y]^2\} \\ =& \{[1 - \frac{1}{4}(1 - \cos k_1\Delta x)]^2 - \frac{\eta^2}{2}(1 - 2\eta^2)(1 - \cos k_1\Delta x)^2\} \\ & \cdot \{[1 - \frac{1}{4}(1 - \cos k_2\Delta y)]^2 - \frac{\phi^2}{2}(1 - 2\phi^2)(1 - \cos k_2\Delta y)^2\} \end{aligned} \tag{4.9}$$

For $|\eta| < \frac{1}{2}$ and $|\phi| < \frac{1}{2}$, the magnitude of the amplification factor, $\left|\frac{\rho^{TD}_{i,j}}{\rho^n_{i,j}}\right|$, in (4.9) is always less than 1. Therefore, the fully two–dimensional transport formula (3.18) is stable under von Neumann's criterion for stability.

To analyze the phase behavior in the transport algorithms, assume $\mathrm{Im}(\rho) = 0$ at time $t = n\Delta t$ and $\vec{r}$ is the position of $\mathrm{Im}(\rho) = 0$ at the end of one cycle. The analytic solution to the phase shift in the constant velocity field is $\vec{r} = \vec{u}\Delta t$ for one time step Δt.

For the one–dimensional transport formula (2.4), the phase shift for one cycle is

$$\tan kx = \frac{\epsilon \sin k\Delta x}{1 - (\frac{1}{4} + \epsilon^2)(1 - \cos k\Delta x)} \tag{4.10}$$

This gives the relative phase error as (see Appendix C, (II))

$$\frac{x - \epsilon\Delta x}{\epsilon\Delta x} \approx k^2\Delta x^2(\frac{\epsilon^2}{6} - \frac{1}{24}) + O(k^4\Delta x^4) \tag{4.11}$$

Equation (4.11) shows that the phases are second–order accurate and the phase errors become fourth order when $|\epsilon| = \frac{1}{2}$.

For the two–dimensional transport formula (3.18), the phase shift for one cycle is (see Appendix C, (III))

$$\tan \vec{k}\cdot\vec{r} = \frac{[1 - (\frac{1}{4} + \eta^2)(1 - \cos k_1\Delta x)]\phi \sin k_2\Delta y + [1 - (\frac{1}{4} + \phi^2)(1 - \cos k_2\Delta y)]\eta \sin k_1\Delta x}{[1 - (\frac{1}{4} + \eta^2)(1 - \cos k_1\Delta x)][1 - (\frac{1}{4} + \phi^2)(1 - \cos k_2\Delta y)] - \eta\phi \sin k_1\Delta x \sin k_2\Delta y} \tag{4.12}$$

Since it is difficult to extract the analog of (4.11) from formula (4.12), we may try to analyze the phase errors by considering some special cases. Firstly, we observe that if either $\eta = 0$ or $\phi = 0$ the right–hand side of the equation (4.12) reduces to the right–hand side of the equation (4.10). This means the relative phase errors for the two–dimensional transport formula (3.18) are second–order accurate if the fluid–element moves in x direction or in y direction alone. Secondly, if take the right–hand side of the equation (4.12) as $H(\eta, \phi)$, then it gives $H(0,0) = 0$. Using the Taylor expansion for functions of two variables and the forward–difference approximation for the first derivatives, we have

$$
\begin{aligned}
H(\eta,\phi) &= H(0,0) + \frac{\partial H(0,0)}{\partial \eta}(\eta - 0) + \frac{\partial H(0,0)}{\partial \phi}(\phi - 0) + \cdots \\
&\approx H(0,0) + \frac{H(\eta,0) - H(0,0)}{\eta - 0}(\eta - 0) + \frac{H(0,\phi) - H(0,0)}{\phi - 0}(\phi - 0) \\
&\approx H(\eta,0) + H(0,\phi) \qquad (4.13)
\end{aligned}
$$

which approximates the sum of the relative phase errors in x direction and in y direction. Thirdly, under the assumption that $\Delta x = \Delta y$, $k_1 = k_2$ and $v = w$, therefore $\eta = \phi$, the relative phase error for the transport formula (3.18) is given as

$$
\frac{\vec{k}\cdot\vec{r} - \vec{k}\cdot\Delta\vec{r}}{\vec{k}\cdot\Delta\vec{r}} \approx k_1^2\Delta x^2(\frac{1}{6}\eta^2 - \frac{1}{24}) + O(k_1^4\Delta x^4) \qquad (4.14)
$$

where $\Delta\vec{r} = (\Delta t)\vec{u}$. Thus, we could conclude that the transport formula (3.18) has relative phase errors which are second–order accurate with respect to the maximum of $k_1\Delta x$ and $k_2\Delta y$.

4.2 Positivity

The positivity underlying FCT means that the sign of the dependent variable ρ must be preserved under the influence of convection alone. A source term may alter the sign of the dependent variable. Near the steep gradient, positivity is particularly important since the convective fluxes tend to make the transported quantities undershoot or overshoot. To ensure positivity, a large diffusive flux of order zero in Δt may be supplemented in the convective stage.

In the one–dimensional case, the FCT transport formula (2.4) can be rewritten as

$$
\rho_i^{TD} = \frac{1}{8}(1+2\epsilon)^2\rho_{i-1}^n + (\frac{3}{4} - \epsilon^2)\rho_i^n + \frac{1}{8}(1+2\epsilon)^2\rho_{i+1}^n \qquad (4.15)
$$

The coefficients in (4.15) are all nonnegative if $|\epsilon| < \frac{1}{2}$, which ensures positivity.

In the two–dimensional case, the transport formula, (3.18), is given by

$$\rho_{i,j}^{TD} = \frac{1}{64}\left\{ \begin{array}{ccc} (1+2\eta)^2(1-2\phi)^2 & 2(3-4\eta^2)(1-2\phi)^2 & (1-2\eta)^2(1-2\phi)^2 \\ 2(1+2\eta)^2(3-4\phi^2) & 4(3-4\eta^2)(3-4\phi^2) & 2(1-2\eta)^2(3-4\phi^2) \\ (1+2\eta)^2(1+2\phi)^2 & 2(3-4\eta^2)(1+2\phi)^2 & (1-2\eta)^2(1+2\phi)^2 \end{array} \right\} \rho_{i,j}^{n}$$

It is clear that all of the coefficients in (3.18) are non–negative if $|\eta| < \frac{1}{2}$ and $|\phi| < \frac{1}{2}$. Consequently, $\rho_{i,j}^{TD} \geq 0$ if all $\rho_{i,j}^{n} \geq 0$, and positivity is preserved.

SECTION 5:

Antidiffusion and Flux Correction in the Two–Dimensional Case

5.1 Fully Two–Dimensional Antidiffusive Scheme

As seen in the previous section, the fully two–dimensional transport scheme is stable and preserves positivity, but has large diffusion. To remove the erroneous diffusion, the zero–velocity diffusion in (3.19) suggests that the removal of an equal and opposite net diffusion from the transported quantity $\{\rho_{i,j}^{TD}\}$ may work, which is given as

$$\rho_{i,j}^{n+1} = \rho_{i,j}^{TD} - \frac{1}{64}\begin{Bmatrix} 1 & 6 & 1 \\ 6 & -28 & 6 \\ 1 & 6 & 1 \end{Bmatrix}\rho_{i,j}^{TD} \tag{5.1}$$

This antidiffusive formula, however, will introduce new maxima and minima near steep gradients which is physically unreasonable and does not maintain positivity. In removing the problem of non–positivity, it is helpful to work with the fluxes directly. Let antidiffusive fluxes be defined as

$$\begin{aligned}
f_{i,j+\frac{1}{2}} &= \frac{6}{64}(\rho_{i,j+1}^{TD} - \rho_{i,j}^{TD}) & f_{i-\frac{1}{2},j+\frac{1}{2}} &= \frac{1}{64}(\rho_{i-1,j+1}^{TD} - \rho_{i,j}^{TD}) \\
f_{i,j-\frac{1}{2}} &= \frac{6}{64}(\rho_{i,j}^{TD} - \rho_{i,j-1}^{TD}) & f_{i+\frac{1}{2},j-\frac{1}{2}} &= \frac{1}{64}(\rho_{i,j}^{TD} - \rho_{i+1,j-1}^{TD}) \\
f_{i+\frac{1}{2},j} &= \frac{6}{64}(\rho_{i+1,j}^{TD} - \rho_{i,j}^{TD}) & f_{i+\frac{1}{2},j+\frac{1}{2}} &= \frac{1}{64}(\rho_{i+1,j+1}^{TD} - \rho_{i,j}^{TD}) \\
f_{i-\frac{1}{2},j} &= \frac{6}{64}(\rho_{i,j}^{TD} - \rho_{i-1,j}^{TD}) & f_{i-\frac{1}{2},j-\frac{1}{2}} &= \frac{1}{64}(\rho_{i,j}^{TD} - \rho_{i-1,j-1}^{TD})
\end{aligned} \tag{5.2}$$

Then the antidiffusive formula (5.1) can be rewritten as

$$\begin{aligned}
\rho_{i,j}^{n+1} = \rho_{i,j}^{TD} - [&f_{i-\frac{1}{2},j+\frac{1}{2}} - f_{i+\frac{1}{2},j-\frac{1}{2}} + f_{i,j+\frac{1}{2}} - f_{i,j-\frac{1}{2}} \\
&+ f_{i+\frac{1}{2},j+\frac{1}{2}} - f_{i-\frac{1}{2},j-\frac{1}{2}} + f_{i+\frac{1}{2},j} - f_{i-\frac{1}{2},j}]
\end{aligned} \tag{5.3}$$

The antidiffusive fluxes in (5.2) must be reduced to maintain positivity of the density $\rho_{i,j}^{n+1}$ in (5.3). This reduction process is called the correction of flux, and gives rise to the

name 'Flux–Corrected Transport' (FCT). To correct the antidiffusive flux, let the corrected flux be

$$f^c_{.,.} = C_{.,.} \cdot f_{.,.} \tag{5.4}$$

and then the corresponding antidiffusive formula in (5.3) becomes

$$\begin{aligned}\rho^{n+1}_{i,j} = \rho^{TD}_{i,j} - [&f^c_{i-\frac{1}{2},j+\frac{1}{2}} - f^c_{i+\frac{1}{2},j-\frac{1}{2}} + f^c_{i,j+\frac{1}{2}} - f^c_{i,j-\frac{1}{2}} \\ &+ f^c_{i+\frac{1}{2},j+\frac{1}{2}} - f^c_{i-\frac{1}{2},j-\frac{1}{2}} + f^c_{i+\frac{1}{2},j} - f^c_{i-\frac{1}{2},j}]\end{aligned} \tag{5.5}$$

We seek to find a flux limiter, $C_{.,.}$ in (5.4), such that the antidiffusive formula (5.5) should not cause the final values of $\{\rho^{n+1}_{i,j}\}$ to be overshoots or undershoots. In the spirit of Zalesak's work [24], the determination of the limiters $\{C_{.,.}\}$ is given by defining

$$\begin{aligned}P^+_{i,j} =& \text{the sum of all antidiffusive fluxes into grid point } (x_i, y_j) \\ =& \max(0, f_{i+\frac{1}{2},j-\frac{1}{2}}) - \min(0, f_{i-\frac{1}{2},j+\frac{1}{2}}) + \max(0, f_{i,j-\frac{1}{2}}) - \min(0, f_{i,j+\frac{1}{2}}) \\ &+ \max(0, f_{i-\frac{1}{2},j-\frac{1}{2}}) - \min(0, f_{i+\frac{1}{2},j+\frac{1}{2}}) + \max(0, f_{i-\frac{1}{2},j}) - \min(0, f_{i+\frac{1}{2},j}) \\ Q^+_{i,j} =& (\rho^{max}_{i,j} - \rho^{TD}_{i,j}) \\ R^+_{i,j} =& \begin{cases} \min(1, \frac{Q^+_{i,j}}{P^+_{i,j}}), & \text{if } P^+_{i,j} > 0 \\ 0 \quad , & \text{if } P^+_{i,j} = 0 \end{cases}\end{aligned} \tag{5.6}$$

and

$$\begin{aligned}P^-_{i,j} =& \text{the sum of all antidiffusive fluxes away from grid point } (x_i, y_j) \\ =& \max(0, f_{i-\frac{1}{2},j+\frac{1}{2}}) - \min(0, f_{i+\frac{1}{2},j-\frac{1}{2}}) + \max(0, f_{i,j+\frac{1}{2}}) - \min(0, f_{i,j-\frac{1}{2}}) \\ &+ \max(0, f_{i+\frac{1}{2},j+\frac{1}{2}}) - \min(0, f_{i-\frac{1}{2},j-\frac{1}{2}}) + \max(0, f_{i+\frac{1}{2},j}) - \min(0, f_{i-\frac{1}{2},j}) \\ Q^-_{i,j} =& (\rho^{TD}_{i,j} - \rho^{min}_{i,j}) \\ R^-_{i,j} =& \begin{cases} \min(1, \frac{Q^-_{i,j}}{P^-_{i,j}}), & \text{if } P^-_{i,j} > 0 \\ 0 \quad , & \text{if } P^-_{i,j} = 0 \end{cases}\end{aligned} \tag{5.7}$$

where the maximum value $\rho_{i,j}^{max}$ and the minimum value $\rho_{i,j}^{min}$ are chosen as follows

$$\rho_{i,j}^{a} = \max(\rho_{i,j}^{TD}, \rho_{i,j}^{n}) \tag{5.8a}$$

$$\rho_{i,j}^{max} = \max(\rho_{i-1,j-1}^{a}, \rho_{i,j-1}^{a}, \rho_{i+1,j-1}^{a}, \rho_{i-1,j}^{a}, \rho_{i,j}^{a}, \rho_{i+1,j}^{a}, \rho_{i-1,j+1}^{a}, \rho_{i,j+1}^{a}, \rho_{i+1,j+1}^{a})$$

$$\rho_{i,j}^{b} = \min(\rho_{i,j}^{TD}, \rho_{i,j}^{n}) \tag{5.8b}$$

$$\rho_{i,j}^{min} = \min(\rho_{i-1,j-1}^{b}, \rho_{i,j-1}^{b}, \rho_{i+1,j-1}^{b}, \rho_{i-1,j}^{b}, \rho_{i,j}^{b}, \rho_{i+1,j}^{b}, \rho_{i-1,j+1}^{b}, \rho_{i,j+1}^{b}, \rho_{i+1,j+1}^{b})$$

These choices of $\rho_{i,j}^{max}$ and $\rho_{i,j}^{min}$ allow us to look back to the previous time step for upper and lower bounds on $\rho_{i,j}^{n+1}$. Since all antidiffusive fluxes are directed away from one grid point into an adjacent one, flux limiting should take place with respect to undershoots for the former and with respect to overshoots for the latter. This demands our taking a minimum to guarantee that neither event comes to pass. Therefore, we define limiters $\{C_{\cdot,\cdot}\}$ to be

$$\begin{aligned}
C_{i,j+\frac{1}{2}} &= \begin{cases} \min(R_{i,j+1}^{+}, R_{i,j}^{-}), & \text{if} \quad f_{i,j+\frac{1}{2}} \geq 0 \\ \min(R_{i,j+1}^{-}, R_{i,j}^{+}), & \text{if} \quad f_{i,j+\frac{1}{2}} < 0 \end{cases} \\
C_{i,j-\frac{1}{2}} &= \begin{cases} \min(R_{i,j}^{+}, R_{i,j-1}^{-}), & \text{if} \quad f_{i,j-\frac{1}{2}} \geq 0 \\ \min(R_{i,j}^{-}, R_{i,j-1}^{+}), & \text{if} \quad f_{i,j-\frac{1}{2}} < 0 \end{cases} \\
C_{i+\frac{1}{2},j} &= \begin{cases} \min(R_{i+1,j}^{+}, R_{i,j}^{-}), & \text{if} \quad f_{i+\frac{1}{2},j} \geq 0 \\ \min(R_{i+1,j}^{-}, R_{i,j}^{+}), & \text{if} \quad f_{i+\frac{1}{2},j} < 0 \end{cases} \\
C_{i-\frac{1}{2},j} &= \begin{cases} \min(R_{i,j}^{+}, R_{i-1,j}^{-}), & \text{if} \quad f_{i-\frac{1}{2},j} \geq 0 \\ \min(R_{i,j}^{-}, R_{i-1,j}^{+}), & \text{if} \quad f_{i-\frac{1}{2},j} < 0 \end{cases} \\
C_{i-\frac{1}{2},j+\frac{1}{2}} &= \begin{cases} \min(R_{i-1,j+1}^{+}, R_{i,j}^{-}), & \text{if} \quad f_{i-\frac{1}{2},j+\frac{1}{2}} \geq 0 \\ \min(R_{i-1,j+1}^{-}, R_{i,j}^{+}), & \text{if} \quad f_{i-\frac{1}{2},j+\frac{1}{2}} < 0 \end{cases} \\
C_{i+\frac{1}{2},j-\frac{1}{2}} &= \begin{cases} \min(R_{i,j}^{+}, R_{i+1,j-1}^{-}), & \text{if} \quad f_{i+\frac{1}{2},j-\frac{1}{2}} \geq 0 \\ \min(R_{i,j}^{-}, R_{i+1,j-1}^{+}), & \text{if} \quad f_{i+\frac{1}{2},j-\frac{1}{2}} < 0 \end{cases} \\
C_{i+\frac{1}{2},j+\frac{1}{2}} &= \begin{cases} \min(R_{i+1,j+1}^{+}, R_{i,j}^{-}), & \text{if} \quad f_{i+\frac{1}{2},j+\frac{1}{2}} \geq 0 \\ \min(R_{i+1,j+1}^{-}, R_{i,j}^{+}), & \text{if} \quad f_{i+\frac{1}{2},j+\frac{1}{2}} < 0 \end{cases} \\
C_{i-\frac{1}{2},j-\frac{1}{2}} &= \begin{cases} \min(R_{i,j}^{+}, R_{i-1,j-1}^{-}), & \text{if} \quad f_{i-\frac{1}{2},j-\frac{1}{2}} \geq 0 \\ \min(R_{i,j}^{-}, R_{i-1,j-1}^{+}), & \text{if} \quad f_{i-\frac{1}{2},j-\frac{1}{2}} < 0 \end{cases}
\end{aligned} \tag{5.9}$$

These limiters $\{C_{\cdot,\cdot}\}$ in (5.9) will correct the antidiffusive fluxes in (5.4) and make (5.5) produce "eventually" a second–order accurate solution without overshoots and undershoots in density $\{\rho_{i,j}^{n+1}\}$ (see the examples in Section 6).

5.2 Using the One–Dimensional FCT Antidiffusive Algorithm.

We observed that the "projection" of the fully two–dimensional transport formula (3.18) onto the x–axis or onto the y–axis actually is just the one–dimensional transport formula (2.4) (see Appendix D). This suggests that the one–dimensional antidiffusive algorithm, (2.7) and (2.8), could be used to antidiffuse the transported quantities $\{\rho_{i,j}^{TD}\}$ separately in the x direction and then in the y direction. The antidiffusion algorithm which follows our fully two–dimensional transport algorithm procedes in the following manner.

(I) Antidiffusion of $\{\rho_{i,j}^{TD}\}$ in the x direction for each y_j as

$$\overline{\rho}_{i,j} = \rho_{i,j}^{TD} - (f_{i+\frac{1}{2},j}^{c} - f_{i-\frac{1}{2},j}^{c}) \tag{5.10}$$

where

$$f_{i+\frac{1}{2},j}^{c} = s \cdot \max[0, \min(s \cdot f_{i-\frac{1}{2},j}\ ,\ \text{“}\tfrac{1}{8}\text{”} \cdot |f_{i+\frac{1}{2},j}|\ ,\ s \cdot f_{i+\frac{3}{2},j})\ ]$$

$$f_{i+\frac{1}{2},j} = \rho_{i+1,j}^{TD} - \rho_{i,j}^{TD}$$

$$s = \operatorname{sign}(f_{i+\frac{1}{2},j})$$

(II) Antidiffusion of $\{\overline{\rho}_{i,j}\}$ in the y direction for each x_i as

$$\rho_{i,j}^{n+1} = \overline{\rho}_{i,j} - (f_{i,j+\frac{1}{2}}^{c} - f_{i,j-\frac{1}{2}}^{c}) \tag{5.11}$$

where

$$f_{i,j+\frac{1}{2}}^{c} = s \cdot \max[0, \min(s \cdot f_{i,j-\frac{1}{2}}\ ,\ \text{“}\tfrac{1}{8}\text{”} \cdot |f_{i,j+\frac{1}{2}}|\ ,\ s \cdot f_{i,j+\frac{3}{2}})\ ]$$

$$f_{i,j+\frac{1}{2}} = \overline{\rho}_{i,j+1} - \overline{\rho}_{i,j}$$

$$s = \operatorname{sign}(f_{i,j+\frac{1}{2}})$$

The order of application of the one–dimensional antidiffusion algorithm in the x and in the y directions has almost no influence on the final results $\{\rho_{i,j}^{n+1}\}$. The "$\frac{1}{8}$" in (5.10) and (5.11) is given in (2.9).

SECTION 6:

Computational Tests for the Fully Two–Dimensional FCT Algorithm

Since the emphasis is on handling the shock or steep gradient solutions to the hyperbolic partial differential equation in (1.1), no boundary effect has been considered in our test problems. To see how well the fully two–dimensional FCT algorithm handles shock problems, two different kinds of initial densities are given in Figure 5 and in Figure 9. Figure 5 has computational grid 50×50. Higher density $\rho = 3$ is given on the grid points (x_i, y_j) where $10 \leq i \leq 25$ and $10 \leq j \leq 25$. Lower density $\rho = 0$ is given on the rest of the grid points. Figure 9 has a 75×75 computational grid. Higher density $\rho = 3$ is given on the region of the circle which is centered at grid point (x_{25}, y_{25}) and has radius 15 grid points. Lower density $\rho = 0$ is given on the rest of the grid points. We move both fluid elements counterclockwise along the sides of an isosceles triangle, as shown in Figure 4, with the constant velocities $\vec{u} =< 2, 1 >$, $\vec{u} =< -1, 1 >$ and $\vec{u} =< -1, -2 >$ on each side. With $\Delta x = \Delta y = 1$, $\Delta t = 0.2$ and 50 cycles for each side, both fluid–elements will move back to their original positions every 150 cycles. Owing to the limitation of CPU time, we have the computation of 300 cycles for the fluid–element in Figure 5, but only have the computation of 150 cycles for the one in Figure 9.

In this thesis, two different kinds of antidiffusion algorithms are presented in Section 5: the fully two–dimensional antidiffusion algorithm in Section 5.1, and the iterated one–dimensional FCT antidiffusion algorithm in Section 5.2. For each given fluid–element, both antidiffusion algorithms are tested. The fluid–element is transported first by the algorithm in Section 3, then followed, respectively, by each antidiffusion algorithm in Section 5 for each time advancement Δt.

For the fluid–element in Figure 5, the computations of 300 cycles are shown, respectively, in Figure 6, which uses the antidiffusion algorithm in Section 5.1, and in Figure 7, which uses the antidiffusion algorithm in Section 5.2. For the fluid–element in Figure 9, the computations of 150 cycles are shown, respectively, in Figure 10, which uses the antidiffusion algorithm in Section 5.1, and in Figure 11, which uses the antidiffusion algorithm in Section 5.2.

We compare our algorithms with the well–known Lax–Wendroff scheme which has second–order accuracy in space and time. The Lax–Wendroff scheme for the hyperbolic equation in the uniform velocity field, $\frac{\partial \rho}{\partial t} + v\frac{\partial \rho}{\partial x} + w\frac{\partial \rho}{\partial y} = 0$, is given as

$$\begin{aligned}
\rho_{i,j}^{n+1} &= [1 + \Delta t\frac{\partial}{\partial t} + \frac{1}{2}(\Delta t)^2\frac{\partial^2}{\partial t^2}]\rho_{i,j}^n \\
&= [1 - \Delta t(v\frac{\partial}{\partial x} + w\frac{\partial}{\partial y}) + \frac{1}{2}(\Delta t)^2(v\frac{\partial}{\partial x} + w\frac{\partial}{\partial y})^2]\rho_{i,j}^n \\
&= \begin{Bmatrix} -\frac{1}{4}\eta\phi & -\frac{1}{2}\phi + \frac{1}{2}\phi^2 & \frac{1}{4}\eta\phi \\ \frac{1}{2}\eta + \frac{1}{2}\eta^2 & 1 - \eta^2 - \phi^2 & -\frac{1}{2}\eta + \frac{1}{2}\eta^2 \\ \frac{1}{4}\eta\phi & \frac{1}{2}\phi + \frac{1}{2}\phi^2 & -\frac{1}{4}\eta\phi \end{Bmatrix} \rho_{i,j}^n
\end{aligned}$$

where $\eta = \frac{\Delta t}{\Delta x}v$ and $\phi = \frac{\Delta t}{\Delta y}w$. Using the same conditions given in the above, for the fluid–element given in Figure 5, the computations of 300 cycles is shown in Figure 8, and for the fluid–element given in Figure 9, the computation of 150 cycles is shown in Figure 12. Both of them produce undershoots and overshoots at the shocks of fluid–elements.

The results in Figures 6, 7, 10 and 11 show that our fully two–dimensional FCT algorithm works fairly well. No overshoot or undershoot has been produced in the final results. The comparisons of Figure 6 and 7 with the result in Figure 8, and Figure 10 and 11 with Figure 12 show that our algorithms are "eventually" at least a second order finite difference scheme. The second antidiffusion formula in Section 5.2 works particularly well because the diffusion introduced in the transport stage is almost totally removed by using the adjustable "$\frac{1}{8}$" in (2.9).

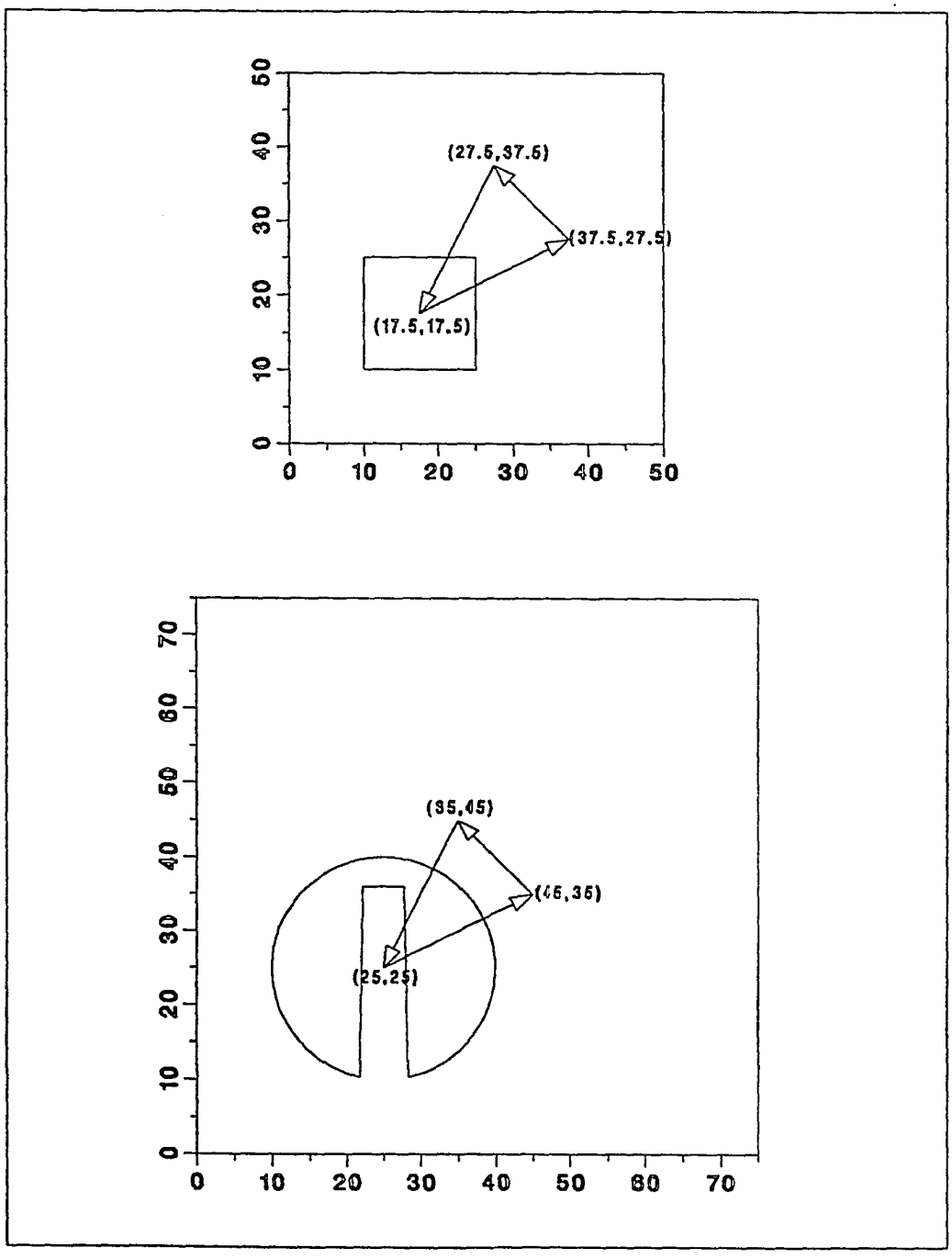

Fig. 4 The locations and the movements of the cubical and the cylindrical fluid–elements on $x-y$ plane in the computational problems.

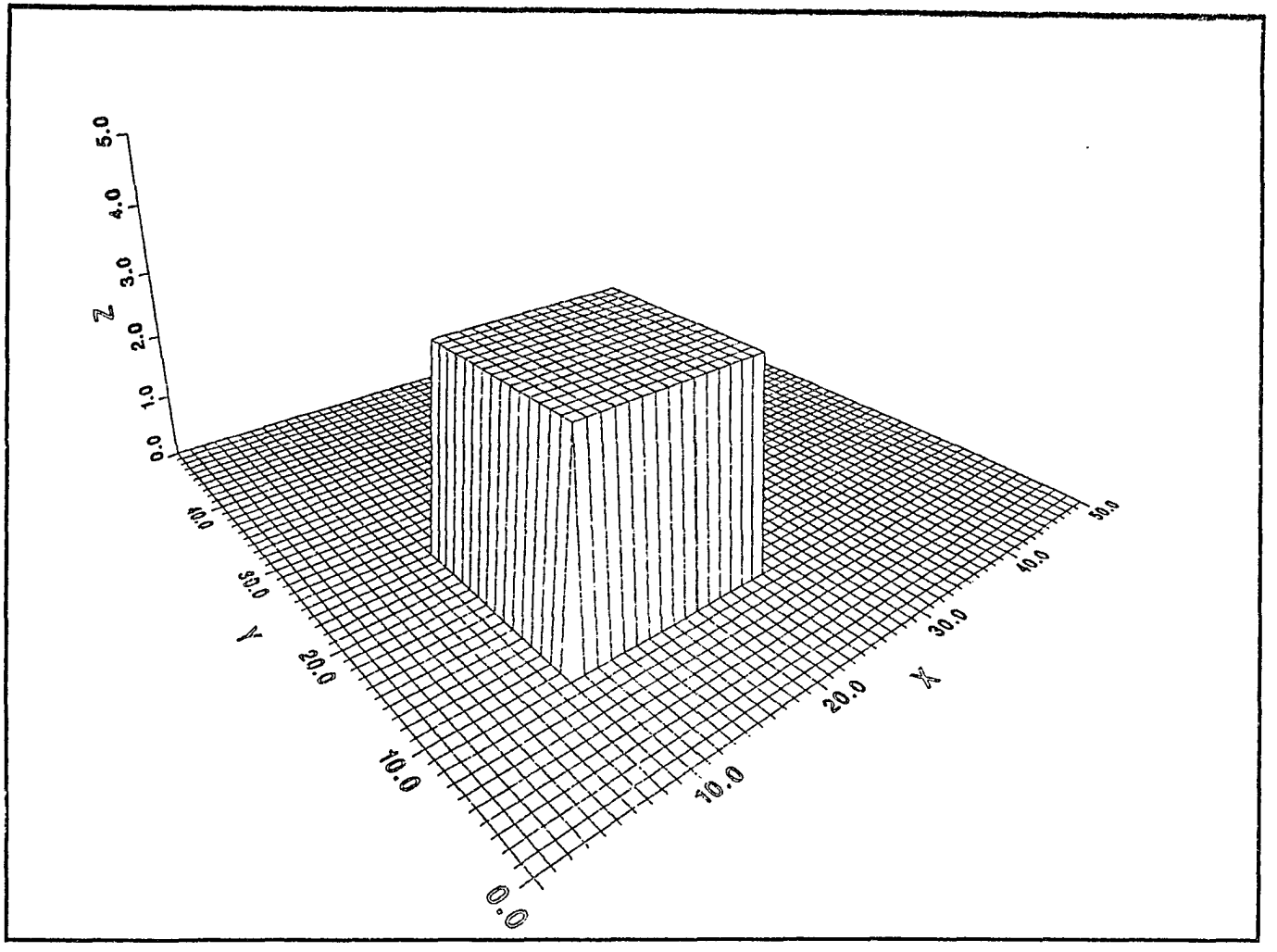

Fig. 5 The initial given cubic fluid–element. It has the density $\rho = 3$ on the region $x_{10} \leq x \leq x_{25}$ and $y_{10} \leq y \leq y_{25}$ and $\rho = 0$ on the rest of the grid points.

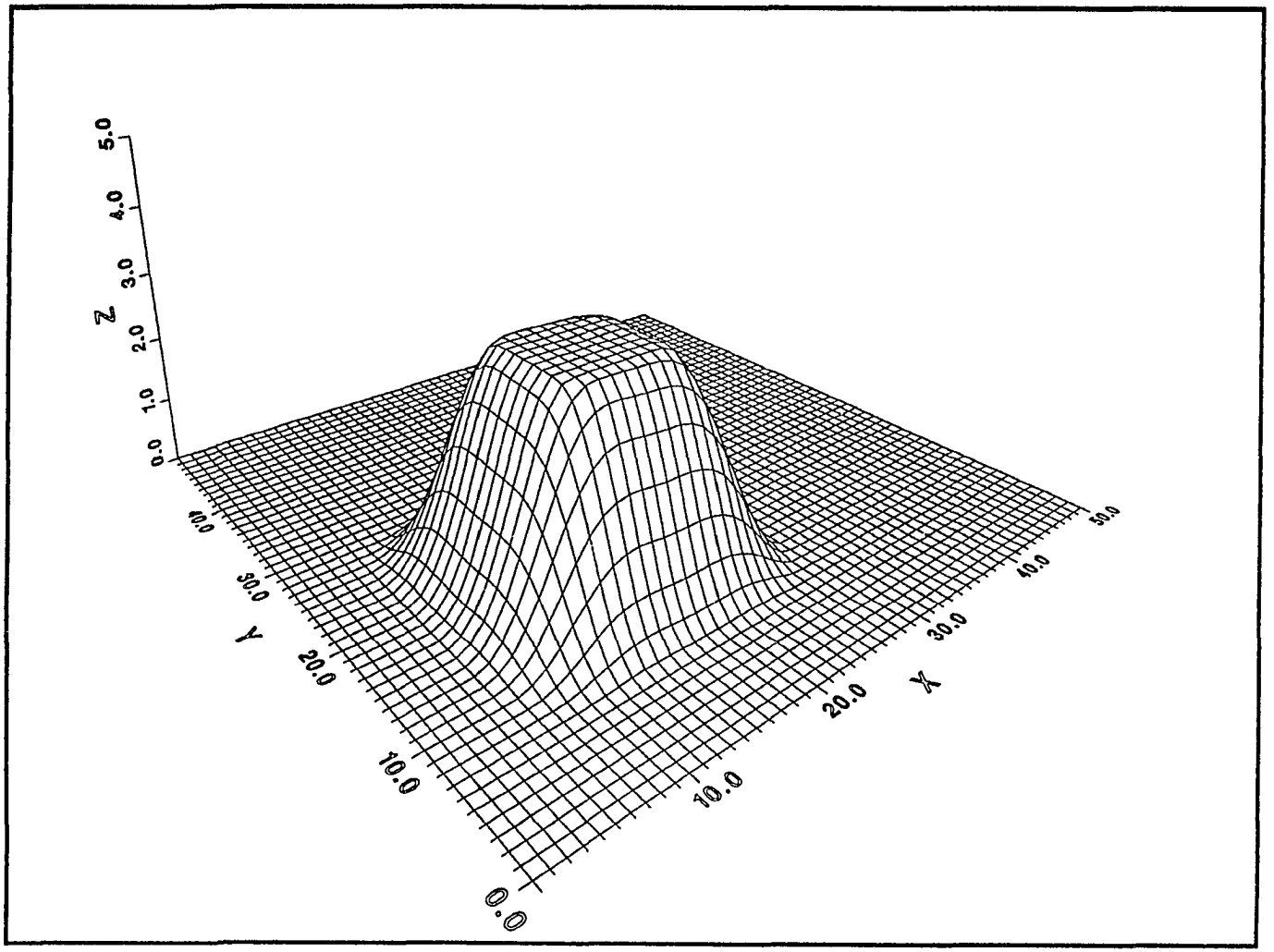

Fig. 6 The result of the transported cubic fluid-element at 300 cycles by using the transport algorithm in Section 3 and the antidiffusive algorithm in Section 5.1 for each cycle. $\Delta t = 0.2$, $\Delta x = \Delta y = 1$ and the movement of the fluid-element is shown in Figure 4.

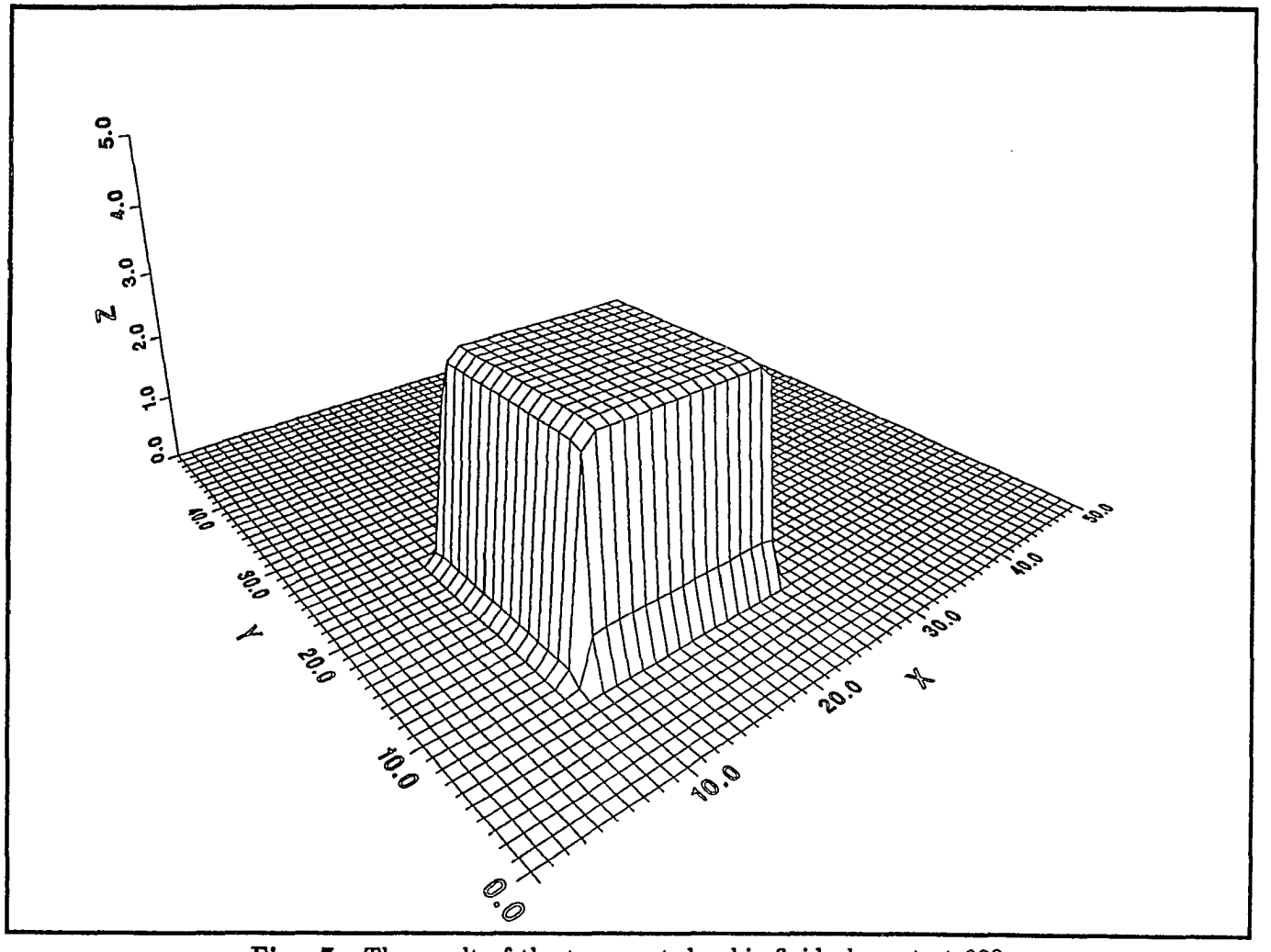

Fig. 7 The result of the transported cubic fluid–element at 300 cycles by using the transport algorithm in Section 3 and the antidiffusive algorithm in Section 5.2 for each cycle. $\Delta t = 0.2$, $\Delta x = \Delta y = 1$ and the movement of the fluid–element is shown in Figure 4.

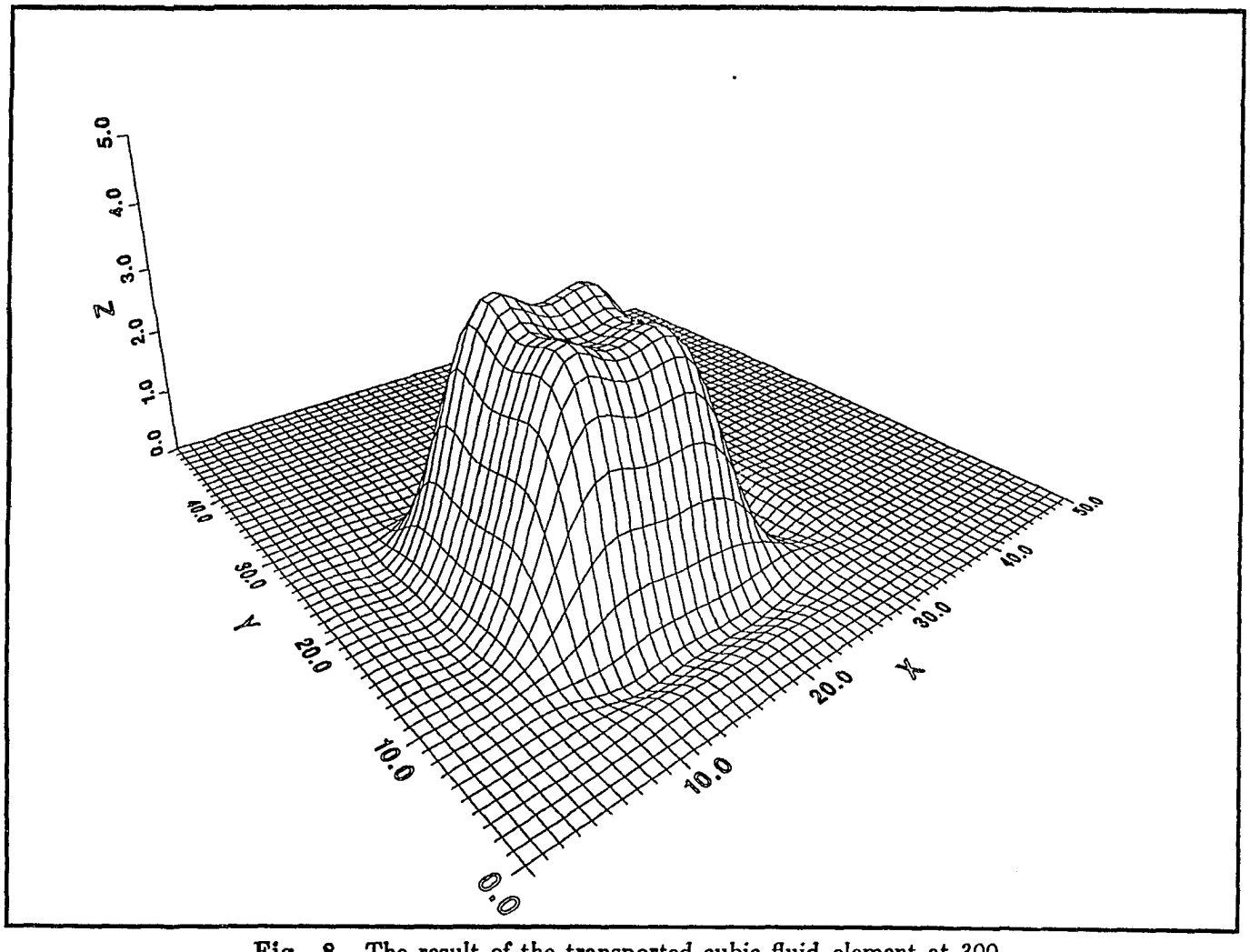

Fig. 8 The result of the transported cubic fluid-element at 300 cycles by using the Lax-Wendroff scheme. $\Delta t = 0.2$, $\Delta x = \Delta y = 1$ and the fluid-element moves as shown in Figure 4.

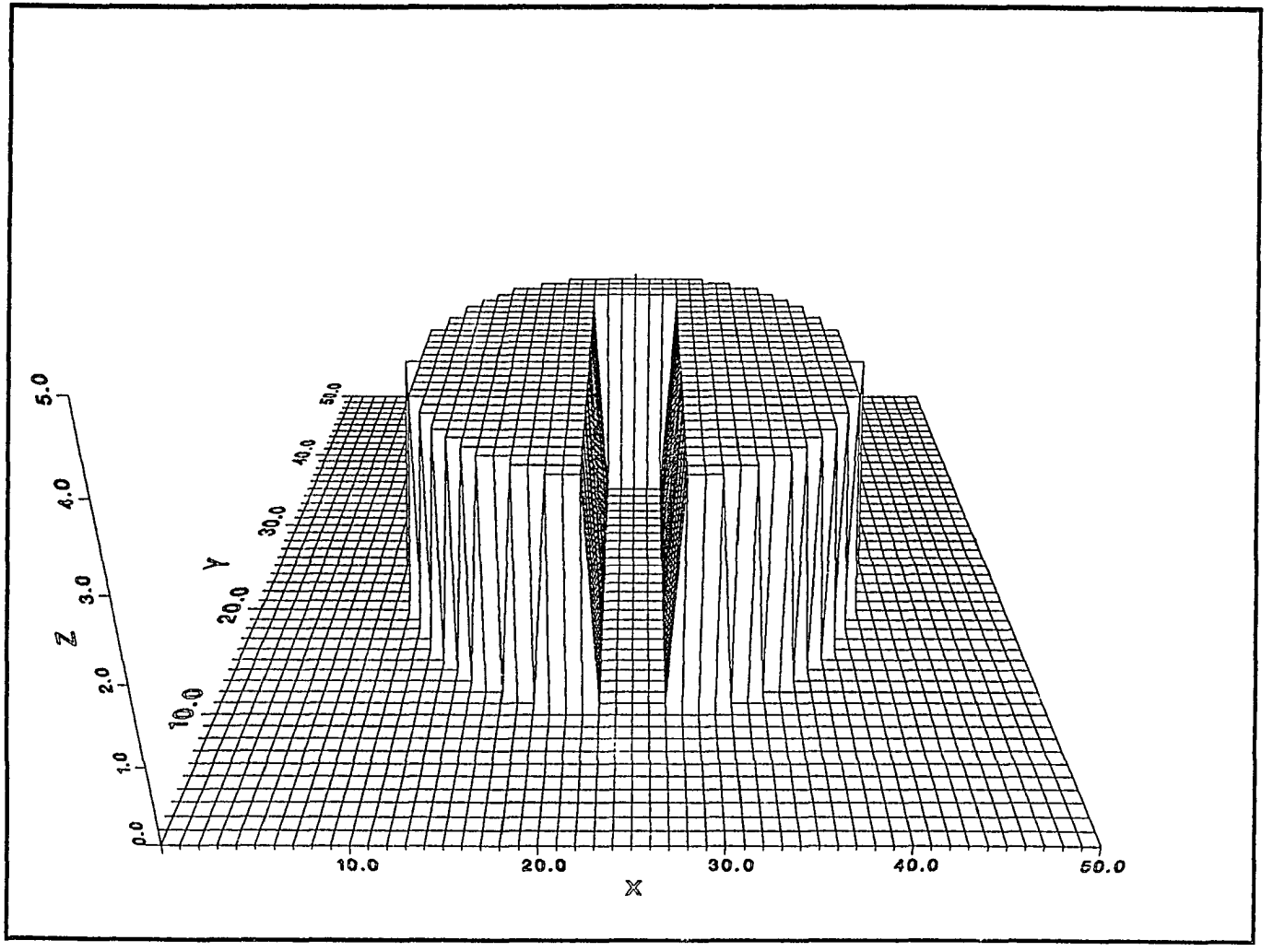

Fig. 9 The initial given cylindrical fluid–element. It has the density $\rho = 3$ on the region of the circle having center at (x_{25}, y_{25}) and the radius 15 grid points, and $\rho = 0$ on the rest of the points.

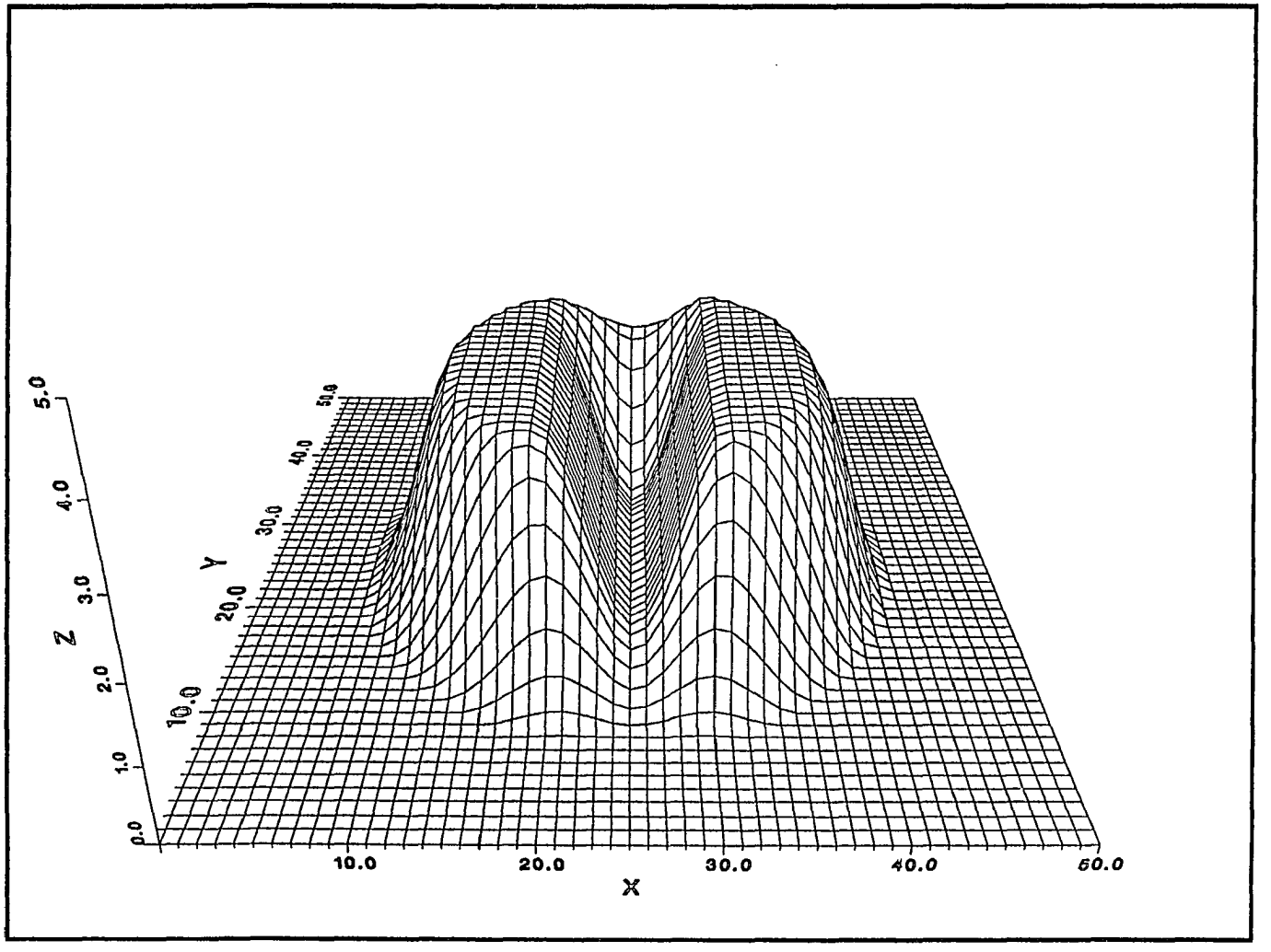

Fig. 10 The result of the transported cylindrical fluid–element at 150 cycles by using the transport algorithm in Section 3 and the antidiffusive algorithm in Section 5.1 for each cycle. $\Delta t = 0.2$, $\Delta x = \Delta y = 1$ and the fluid–element moves as shown in Figure 4.

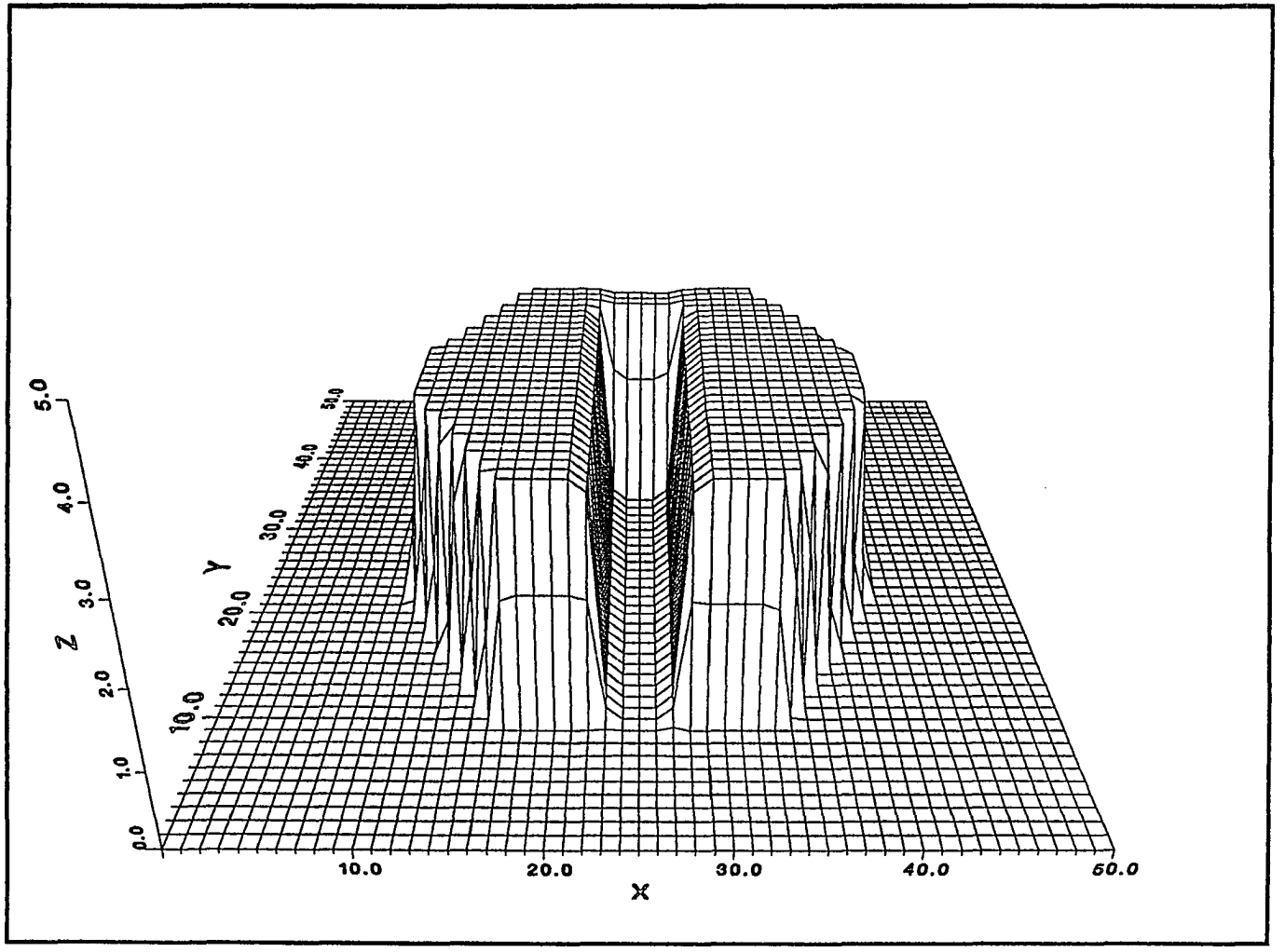

Fig. 11 The result of the transported cylindrical fluid–element at 150 cycles by using the transport algorithm in Section 3 and the antidiffusive algorithm in Section 5.2 for each cycle. $\Delta t = 0.2$, $\Delta x = \Delta y = 1$ and the fluid–element moves as shown in Figure 4.

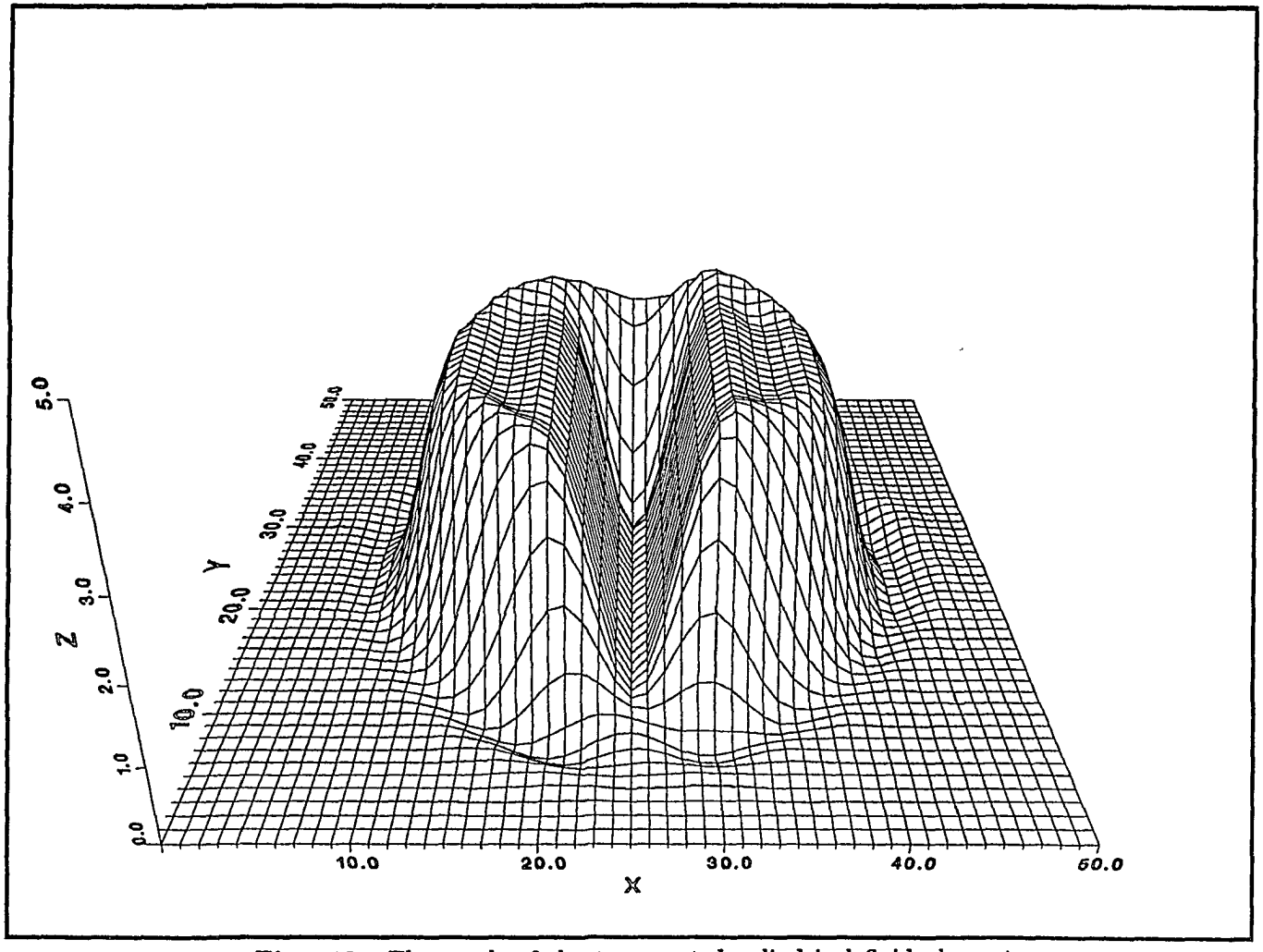

Fig. 12 The result of the transported cylindrical fluid-element at 150 cycles by using the Lax–Wendroff scheme. $\Delta t = 0.2$, $\Delta x = \Delta y = 1$ and the fluid-element moves as shown in Figure 4.

SECTION 7:

Conclusion and Conjecture

The fully two–dimensional FCT algorithm developed in this thesis is positive, stable, mass–conservative and actually second–order accurate as shown above. It produces the final results without the spurious oscillations associated with the more classical second–order schemes. This fully two–dimensional FCT algorithm is only the principal structure for the two–dimensional case. It could be refined by analyzing the phase and amplitude errors and reducing these erroneous diffusions in the antidiffusion stage as Boris and Book did for one–dimensional FCT in [4].

Recently, capturing the schocks for the hyperbolc conservation equations has been investigated by using the flux limiter in the antidiffusive stage(see [8,9,12,13,14,16,17,18,19,20, 22,23]). Harten [12] introduced the notion of TVD (Total Variation Dimishing) to characterize oscillation–free schemes. The TVD constraint on the limiter assures the stability of the resulting scheme using such a limiter. Sweby [20] reorganized the Lax–Wendroff scheme as the first–order scheme plus an antidiffusive flux. He imposed different kinds of limiters on the antidiffusive flux in the Lax–Wendroff scheme and showed that, under the TVD constraint, most of the single–step approach schemes, by using the limiter, fall into the framework of the "modified" Lax–Wendroff schemes. The FCT algorithms are different from the framework of the schemes proposed by Sweby since they are essentially a two–step procedure. However, it suggests that a framework of two–step schemes using limiters could be investigated to refine our two–dimensional FCT algorithm.

In the one–dimensional transport scheme in Section 2, linear interpolation is used throughout the transport stage, which is

$$\rho(x) = A + Bx \quad \text{or} \quad \rho(x) = (1-t)\,\rho(x_i) + t\,\rho(x_{i+1}) \tag{7.1}$$

where

$$t = \frac{(x - x_i)}{(x_{i+1} - x_i)} \quad \text{for} \quad x_i \le x \le x_{i+1}$$

Instead of this linear interpolation, however, it is possible to interpolate the densities by

$$\rho(x) = (1 - t^m)\rho(x_i) + t^m \rho(x_{i+1}) \quad \text{for} \quad m > 0 \tag{7.2}$$

Let $\Delta x = 1$, $\Delta t = 0.2$ and $u = 1$. With the periodic boundaries, the transport schemes for $m = \frac{1}{2}$, 1 and 2 are shown in Figures 13, 14 and 15 respectively. As seen in these figures, the convections of densities in the cases of $m = \frac{1}{2}$ and 2 are slower and faster respectively than in the case of $m = 1$. Similarly, this may happen in the two–dimensional case. Thus, we have $Z(x,y) = A + Bx + Cy + Dxy$ to be the natural way to interpolate the densities on the grid cell, $R_{i+\frac{1}{2},j+\frac{1}{2}}$ in (3.2), in the fully two–dimensional transport scheme.

In the three–dimensional case, if we could cope with the difficulty of the integration in three dimensions, a fully three–dimensional transport algorithm could be found based on the interpolation of densities on the grid cell

$$R_{i+\frac{1}{2},j+\frac{1}{2},k+\frac{1}{2}} = \{\,(x,y,z) \mid \quad x_i \le x \le x_{i+1}, y_j \le y \le y_{j+1}, z_k \le z \le z_{k+1} \quad \}$$

by

$$\rho(x,y,z) = A + Bx + Cy + Dz + Exy + Fyz + Gzx + Hxyz$$

The fully three–dimensional antidiffusion scheme could also be found based on the spirit of Zalesak's work in [24] or just using the one–dimensional antidiffusive algorithm in the x direction, y direction and z direction separately.

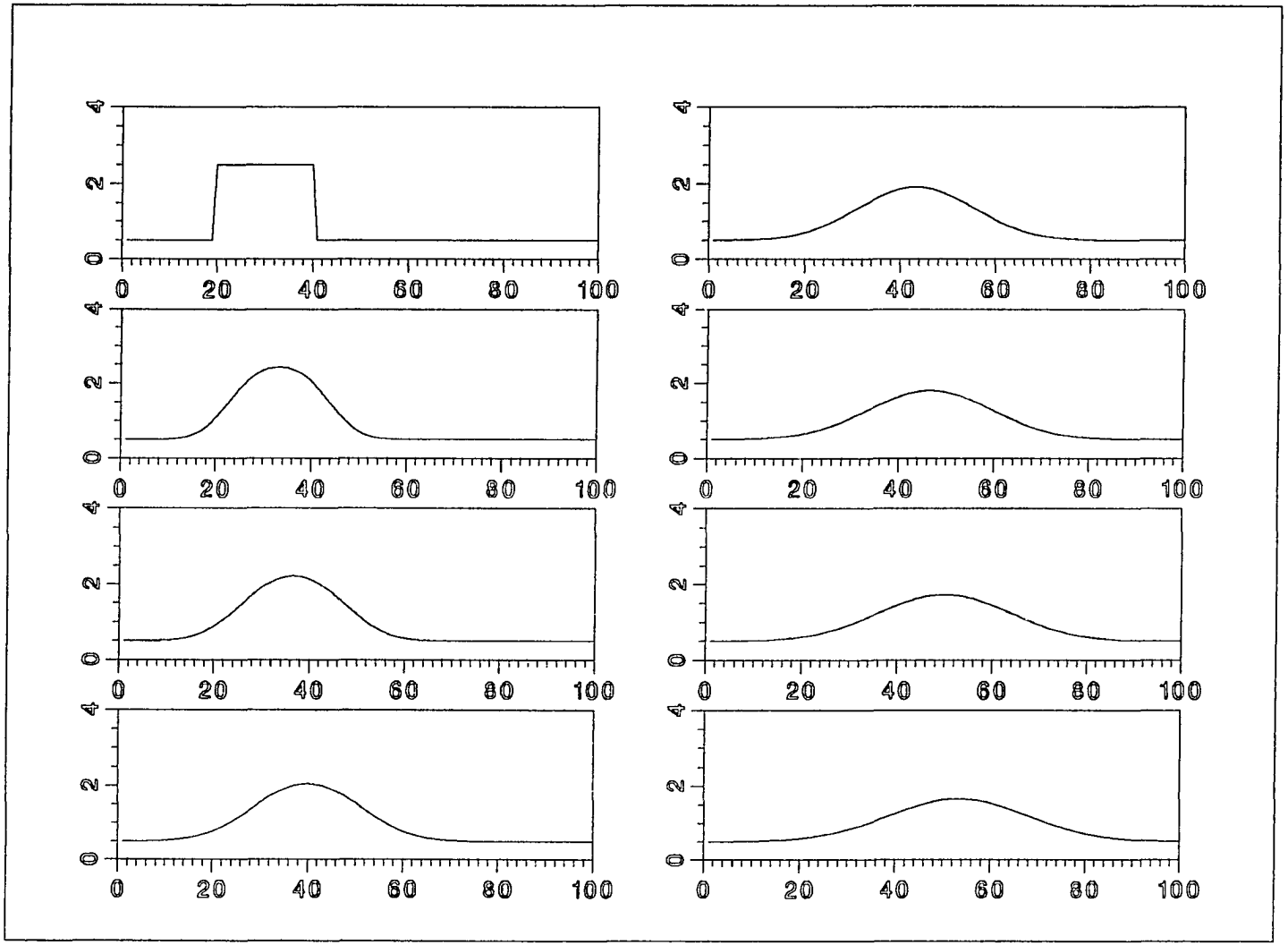

Fig. 13 The transport of the square wave by using the transport scheme (7.2) with $m = \frac{1}{2}$ in (7.2). Data are ploted every 100 cycles.

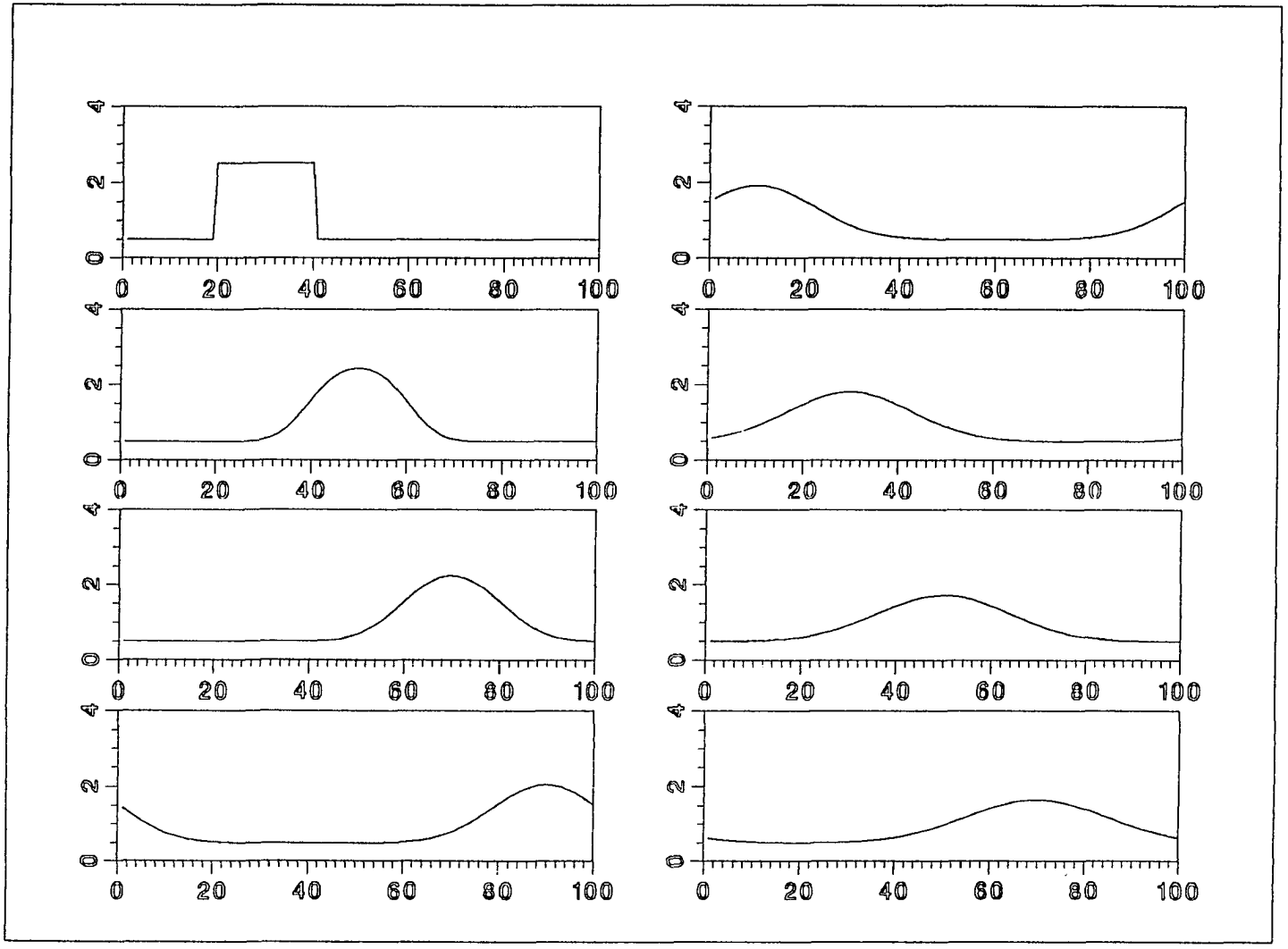

Fig. 14 The transport of the square wave by using the transport scheme (7.2) with $m = 1$ in (7.2). Data are ploted every 100 cycles.

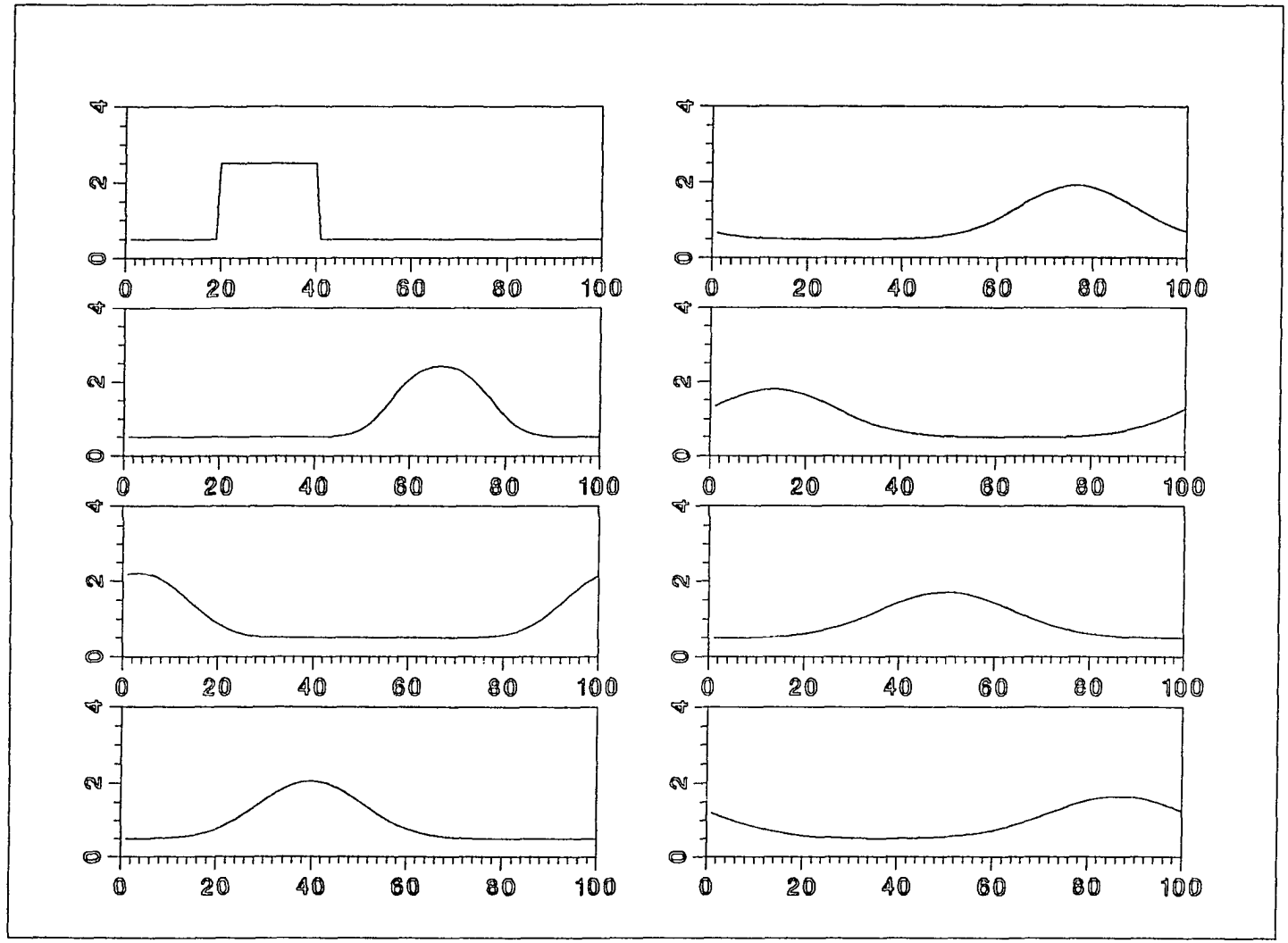

Fig. 15 The transport of the square wave by using the transport scheme (7.2) with $m = 2$ in (7.2). Data are ploted every 100 cycles.

REFERENCES

[1] D.L. Book, J.P. Boris and K. Hain, 1975: Flux–Corrected Transport II: Generalizations Of The Method, *J. of Comp. Phys.*, **18**, pp. 248–283.

[2] J.P. Boris, 1972: SHAS2D, A Fully Compressible Hydrodynamics Code In Two Dimensions, NRL Memorandum Report 2542, Naval Research Labortory.

[3] J.P. Boris and D.L. Book, 1973: Flux–Corrected Transport, I. SHASTA, A Fluid Transport That Works, *J. of Comp. Phys.*, **11**, pp. 38–69.

[4] J.P. Boris and D.L. Book, 1976: Flux–Corrected Transport III: Minimal Error FCT Algorithms, *J. of Comp. Phys.*, **20**, pp. 397–431.

[5] J.P. Boris and D.L. Book, 1976: Solution of Continuity Equations By The Method Of Flux–Corrected Transport, Ch. 11, Vol. 16, Method of Comp. Phys., Academic Press, New York, pp. 85–129.

[6] J.P. Boris, 1976: Flux–Corrected Transport Modules For Solving Generalized Continuity Equations, NRL Memorandum Report 3237, Naval Research Labortory.

[7] Y. Brenier and S. Osher, 1988: The Discrete One–Sided Lipschitz Condition For Convex Scalar Conservation Laws, *SIAM J. Numer. Anal.*, **Vol 25**, pp. 8–23.

[8] S.F. Davis, 1986: Shock Capturing, Numerical Methods For PDE, π Pitman Research Notes In Mathematical Series 145, Longman Scientific & Technical, Chapter 5, pp. 175–197.

[9] B. Engquist and S. Osher, 1981: One–Sided Difference Approximations For Nonlinear Conservation Laws, *Mathematics of Computation*, **Vol. 36**, pp. 321–351.

[10] S.J. Farlow, 1982: Partial Differential Equation For Scientists & Enfineers, John Wiley & Sons, Inc., 402 pp.

[11] R.H. Guirguis, 1983: Two–Dimensional Flux–Corrected Transport, JAYCOR Report Number J206–83–003/6201

[12] A. Harten and P. Lax, 1981: A Random Choice Finite Difference Scheme For Hyperbolic Conservation Law, *SIAM J. Numer. Anal.*, **Vol 18**, pp. 289–315.

[13] A. Harten, 1984: On A Class Of High Resolution Total–Variation–Stable Finite Difference Schemes, *SIAM J. Numer. Anal.*, **Vol 21**, pp. 1–23.

[14] A. Harten and S. Osher, 1987: Uniformly High–Order Accurate Nonosciliatory Schemes. I, *SIAM J. Numer. Anal.*, **Vol 24**, pp. 279–309.

[15] A.R. Mitchell and D.F. Griffiths, 1985: The Finite Difference Method In Partial Differential Equations, A Willey Intersciences Publication, 272 pp.

[16] S. Osher and F. Solomon, 1982: Upwind Difference Schemes For Hyperbolic Systems Of conservation Laws, *Mathematics of Computation*, **Vol. 38**, pp. 339–374.

[17] S. Osher and S. Chakravarthy, 1984: High Resolution Schemes And The Entropy Condition, *SIAM J. Numer. Anal.*, **Vol 21**, pp. 955–984.

[18] S. Osher, 1984: Riemann Solver, The Entropy Condition, And Difference Approximations, *SIAM J. Numer. Anal.*, **Vol 21**, pp. 217–235.

[19] S. Osher and E. Tadmor, 1988: On The Convergence Of Difference Approximations To Scalar Conservation Laws, *Mathematics of Computation*, **Vol. 50**, pp. 19–51.

[20] P.K. Sweby, 1984: High Resolution Schemes Using Flux Limiter For Hyperbolic Conservation Law, *SIAM J. Numer. Anal.*, **Vol. 21**, pp. 995–1011.

[21] E. Tadmor, 1984: The Large–Time Behavior Of The Scalar, Genuinely Nonlinear Lax–Friedrichs Scheme, *Mathematics of Computation*, **Vol. 43**, pp. 353–368.

[22] E. Tadmor, 1984: Numerical Viscosity And The Entropy Condition For Conservative Difference Schemes, *Mathematics of Computation*, **Vol. 43**, pp. 369–381.

[23] J.P. Vila, 1988: High–Order Schemes And Entropy Condition For Nonlinear Hyperbolic Systems Of Conservation Laws, *Mathematics of Computation*, **Vol. 50**, pp. 53–73.

[24] S.T. Zalesak, 1979: Fully Multidimensional Flux–Corrected Transport Algorithms For Fluids, *J. of Comp. Phys.*, **31**, pp. 335–362.

APPENDIX A

Double Integral in the Lemma

§ Lemma: Let R={the region enclosed by quadrilateral having the four vertices,

$$(x_1, y_1),\ (x_2, y_2),\ (x_3, y_3) \text{ and } (x_4, y_4)\ \}$$

then we have

$$\begin{aligned}
\int\int 1\,dR &= \frac{1}{2}[(x_1 - x_3)(y_2 - y_4) + (x_2 - x_4)(y_3 - y_1)] \\
\int\int x\,dR &= \frac{1}{6}[y_1(x_4^2 + x_4x_1 - x_1x_2 - x_2^2) + y_2(x_1^2 + x_1x_2 - x_2x_3 - x_3^2) \\
&\quad + y_3(x_2^2 + x_2x_3 - x_3x_4 - x_4^2) + y_4(x_3^2 + x_3x_4 - x_4x_1 - x_1^2)] \\
\int\int y\,dR &= \frac{1}{6}[x_1(-y_4^2 - y_4y_1 + y_1y_2 + y_2^2) + x_2(-y_1^2 - y_1y_2 + y_2y_3 + y_3^2) \\
&\quad + x_3(-y_2^2 - y_2y_3 + y_3y_4 + y_4^2) + x_4(-y_3^2 - y_3y_4 + y_4y_1 + y_1^2)] \\
\int\int xy\,dR &= \frac{1}{24}[x_1^2(-y_4^2 - 2y_4y_1 + 2y_1y_2 + y_2^2) + x_2^2(-y_1^2 - 2y_1y_2 + 2y_2y_3 + y_3^2) \\
&\quad + x_3^2(-y_2^2 - 2y_2y_3 + 2y_3y_4 + y_4^2) + x_4^2(-y_3^2 - 2y_3y_4 + 2y_4y_1 + y_1^2) \\
&\quad + 2x_1x_2(-y_1^2 + y_2^2) + 2x_2x_3(-y_2^2 + y_3^2) + 2x_3x_4(-y_3^2 + y_4^2) \\
&\quad + 2x_4x_1(-y_4^2 + y_1^2)]
\end{aligned}$$

Proof:

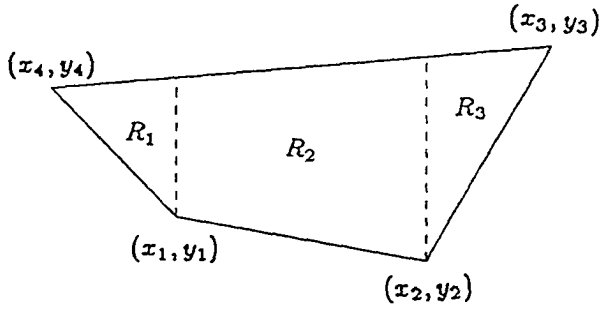

As seen in the above graph, the double integral of $f(x, y)$ over the region R is performed

as the sum of the three subintegrals,

$$\begin{aligned}\int\int f(x,y)\,dR &= \int\int f(x,y)\,dR_1 + \int\int f(x,y)\,dR_2 + \int\int f(x,y)\,dR_3 \\ &= \int_{x_1}^{x_4}\int_{y_4+\frac{y_1-y_4}{x_1-x_4}(x-x_4)}^{y_3+\frac{y_4-y_3}{x_4-x_3}(x-x_3)} f(x,y)\,dydx \\ &\quad + \int_{x_2}^{x_1}\int_{y_1+\frac{y_2-y_1}{x_2-x_1}(x-x_1)}^{y_3+\frac{y_4-y_3}{x_4-x_3}(x-x_3)} f(x,y)\,dydx \\ &\quad + \int_{x_3}^{x_2}\int_{y_2+\frac{y_3-y_2}{x_3-x_2}(x-x_2)}^{y_3+\frac{y_4-y_3}{x_4-x_3}(x-x_3)} f(x,y)\,dydx\end{aligned}$$

The substutions of the functions $f(x,y) = 1$, x, y and xy into the integral can be simplified to the results as shown in the lemma. Since the results are independent of the positions of the four vertices, the proof is without loss of generality.

APPENDIX B

The Fully 2D Transport Formula for a Uniform–Velocity Field

The complete transport algorithm which relates $\{\rho_{i,j}^{TD}\}$ to $\{\rho_{i,j}^{n}\}$ in the uniform velocity field $\vec{u} =< v, w >$, is

$$\rho_{i,j}^{TD} = \frac{1}{64} \left\{ \begin{array}{ccc} (1+2\eta)^2(1-2\phi)^2 & 2(3-4\eta^2)(1-2\phi)^2 & (1-2\eta)^2(1-2\phi)^2 \\ 2(1+2\eta)^2(3-4\phi^2) & 4(3-4\eta^2)(3-4\phi^2) & 2(1-2\eta)^2(3-4\phi^2) \\ (1+2\eta)^2(1+2\phi)^2 & 2(3-4\eta^2)(1+2\phi)^2 & (1-2\eta)^2(1+2\phi)^2 \end{array} \right\} \rho_{i,j}^{n}$$

where $\eta \equiv \frac{\Delta t}{\Delta x} v$ and $\phi \equiv \frac{\Delta t}{\Delta y} w$.

Proof:

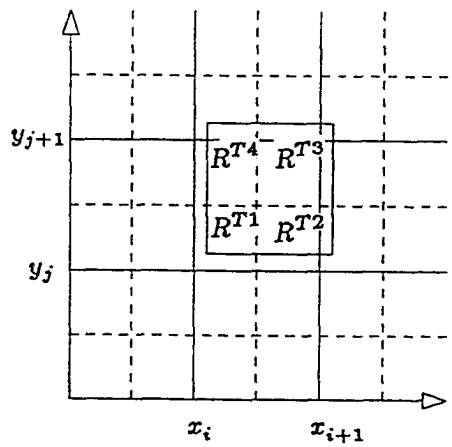

Consider the transport of the fluid–element on the grid cell $R_{i+\frac{1}{2},j+\frac{1}{2}}$ for one time step advancement Δt, where $R_{i+\frac{1}{2},j+\frac{1}{2}}$ is defined in (3.2). Let $\vec{r} =< x, y >$. Four grid points, (x_i, y_j), (x_{i+1}, y_j), (x_{i+1}, y_{j+1}) and (x_i, y_{j+1}), as shown in the above graph, move to the new positions at the end of the transport by the formula $\vec{r}^{new} = \vec{r}^{old} + \vec{u}\Delta t$. Since the velocity $\vec{u}$ is a constant all the time during transport, we have κ in (3.14) equal to 1 and

$\rho^T_{i,j} = \rho^n_{i,j}$ in (3.15). The interpolation (3.7) of the transported density on the transported area $R^T_{i+\frac{1}{2},j+\frac{1}{2}}$ reduces to the equation

$$\begin{vmatrix} 1 & x & y & xy & Z^T \\ 1 & x_i + \Delta tv & y_j + \Delta tw & (x_i + \Delta tv)(y_j + \Delta tw) & \rho^n_{i,j} \\ 1 & x_{i+1} + \Delta tv & y_j + \Delta tw & (x_{i+1} + \Delta tv)(y_j + \Delta tw) & \rho^n_{i+1,j} \\ 1 & x_{i+1} + \Delta tv & y_{j+1} + \Delta tw & (x_{i+1} + \Delta tv)(y_{j+1} + \Delta tw) & \rho^n_{i+1,j+1} \\ 1 & x_i + \Delta tv & y_{j+1} + \Delta tw & (x_i + \Delta tv)(y_{j+1} + \Delta tw) & \rho^n_{i,j+1} \end{vmatrix} = 0$$

or

$$\begin{aligned} Z^T(x,y) = \frac{1}{\Delta x \Delta y}\{&\rho^n_{i,j}[x - (x_{i+1} + \Delta tv)][y - (y_{j+1} + \Delta tw)] \\ &- \rho^n_{i+1,j}[x - (x_i + \Delta tv)][y - (y_{j+1} + \Delta tw)] \\ &+ \rho^n_{i+1,j+1}[x - (x_i + \Delta tv)][y - (y_j + \Delta tw)] \\ &- \rho^n_{i,j+1}[x - (x_{i+1} + \Delta tv)][y - (y_j + \Delta tw)]\} \end{aligned}$$

The subvolumes, $V^{TI}_{i+\frac{1}{2},j+\frac{1}{2}}$, I=1, 2, 3 and 4, of the transported fluid–element in (3.10) are computed as follows

$$\begin{aligned} V^{T1}_{i+\frac{1}{2},j+\frac{1}{2}} &= \int\int Z^T \, dR^{T1}_{i+\frac{1}{2},j+\frac{1}{2}} \\ &= \int_{x_i+\Delta tv}^{x_i+\frac{1}{2}\Delta x} \int_{y_j+\Delta tw}^{y_j+\frac{1}{2}\Delta y} Z^T \, dydx \\ &= \frac{1}{64}\Delta x \Delta y\{\rho^n_{i,j}[4 - (1+2\eta)^2][4 - (1+2\phi)^2] + \rho^n_{i+1,j}(1-2\eta)^2[4 - (1+2\phi)^2] \\ &\quad + \rho^n_{i+1,j+1}(1-2\eta)^2(1-2\phi)^2 + \rho^n_{i,j+1}[4 - (1+2\eta)^2](1-2\phi)^2\} \end{aligned}$$

$$\begin{aligned} V^{T2}_{i+\frac{1}{2},j+\frac{1}{2}} &= \int\int Z^T \, dR^{T2}_{i+\frac{1}{2},j+\frac{1}{2}} \\ &= \int_{x_i+\frac{1}{2}\Delta x}^{x_{i+1}+\Delta tv} \int_{y_j+\Delta tw}^{y_j+\frac{1}{2}\Delta y} Z^T \, dydx \\ &= \frac{1}{64}\Delta x \Delta y\{\rho^n_{i,j}(1+2\eta)^2[4 - (1+2\phi)^2] + \rho^n_{i+1,j}[4 - (1-2\eta)^2][4 - (1+2\phi)^2] \\ &\quad + \rho^n_{i+1,j+1}[4 - (1-2\eta)^2](1-2\phi)^2 + \rho^n_{i,j+1}(1+2\eta)^2(1-2\phi)^2\} \end{aligned}$$

$$V^{T3}_{i+\frac{1}{2},j+\frac{1}{2}} = \int\int Z^T \, dR^{T3}_{i+\frac{1}{2},j+\frac{1}{2}}$$
$$= \int_{x_i+\frac{1}{2}\Delta x}^{x_{i+1}+\Delta tv} \int_{y_j+\frac{1}{2}\Delta x}^{y_{j+1}+\Delta tw} Z^T \, dydx$$
$$= \frac{1}{64}\Delta x\Delta y\{\rho^n_{i,j}(1+2\eta)^2(1+2\phi)^2 + \rho^n_{i+1,j}[4-(1-2\eta)^2](1+2\phi)^2$$
$$+ \rho^n_{i+1,j+1}[4-(1-2\eta)^2][4-(1-2\phi)^2] + \rho^n_{i,j+1}(1+2\eta)^2[4-(1-2\phi)^2]\}$$

$$V^{T4}_{i+\frac{1}{2},j+\frac{1}{2}} = \int\int Z^T \, dR^{T4}_{i+\frac{1}{2},j+\frac{1}{2}}$$
$$= \int_{x_i+\Delta tv}^{x_i+\frac{1}{2}\Delta x} \int_{y_j+\frac{1}{2}\Delta y}^{y_{j+1}+\Delta tw} Z^T \, dydx$$
$$= \frac{1}{64}\Delta x\Delta y\{\rho^n_{i,j}[4-(1+2\eta)^2](1+2\phi)^2 + \rho^n_{i+1,j}(1-2\eta)^2(1+2\phi)^2$$
$$+ \rho^n_{i+1,j+1}(1-2\eta)^2[4-(1-2\phi)^2] + \rho^n_{i,j+1}[4-(1+2\eta)^2][4-(1-2\phi)^2]\}$$

Next, sum up all of the subvolumes over $R_{i,j}$, where $R_{i,j}$ is defined in (3.17), as

$$V_{i,j} = V^{T1}_{i+\frac{1}{2},j+\frac{1}{2}} + V^{T2}_{i-\frac{1}{2},j+\frac{1}{2}} + V^{T3}_{i-\frac{1}{2},j-\frac{1}{2}} + V^{T4}_{i+\frac{1}{2},j-\frac{1}{2}}$$

This gives the transported density back onto the grid point (x_i, y_j) as

$$\rho^{TD}_{i,j} = \frac{V_{i,j}}{\Delta x\Delta y}$$

or

$$\rho^{TD}_{i,j} = \frac{1}{64}\begin{Bmatrix} (1+2\eta)^2(1-2\phi)^2 & 2(3-4\eta^2)(1-2\phi)^2 & (1-2\eta)^2(1-2\phi)^2 \\ 2(1+2\eta)^2(3-4\phi^2) & 4(3-4\eta^2)(3-4\phi^2) & 2(1-2\eta)^2(3-4\phi^2) \\ (1+2\eta)^2(1+2\phi)^2 & 2(3-4\eta^2)(1+2\phi)^2 & (1-2\eta)^2(1+2\phi)^2 \end{Bmatrix} \rho^n_{i,j}$$

APPENDIX C

Equations for the Amplification Factor and Phase Shift

(I) Substitution of (4.7) into (3.18) gives

$$
\begin{aligned}
&\rho_{i,j}^{TD} \\
&= \{\frac{1}{8}(1-2\phi)^2\{\frac{1}{8}[(1+2\eta)^2 e^{-\iota k_1\Delta x} + 2(3-4\eta^2) + (1-2\eta)^2 e^{\iota k_1\Delta x}]e^{\iota k_1 i\Delta x}\}e^{-\iota k_2(j+1)\Delta y} \\
&+ \frac{2}{8}(3-4\phi^2)\{\frac{1}{8}[(1+2\eta)^2 e^{-\iota k_1\Delta x} + 2(3-4\eta^2) + (1-2\eta)^2 e^{\iota k_1\Delta x}]e^{\iota k_1 i\Delta x}\}e^{-\iota k_2 j\Delta y} \\
&+ \frac{1}{8}(1+2\phi)^2\{\frac{1}{8}[(1+2\eta)^2 e^{-\iota k_1\Delta x} + 2(3-4\eta^2) + (1-2\eta)^2 e^{\iota k_1\Delta x}]e^{\iota k_1 i\Delta x}\}e^{-\iota k_2(j-1)\Delta y} \\
&\} \cdot e^{-\iota(k_1 vn\Delta t + k_2 wn\Delta t)} \\
&= \{[1-(\frac{1}{4}+\eta^2)(1-\cos k_1\Delta x) - \iota\eta\sin k_1\Delta x]e^{\iota k_1 i\Delta x}\}\times \\
&\{\frac{1}{8}[(1+2\phi)^2 e^{-\iota k_2\Delta y} + 2(3-4\phi^2) + (1-2\phi)^2 e^{\iota k_2\Delta y}]e^{-\iota k_2 j\Delta y}\} \cdot e^{-\iota(k_1 vn\Delta t + k_2 wn\Delta t)} \\
&= \{[1-(\frac{1}{4}+\eta^2)(1-\cos k_1\Delta x) - \iota\eta\sin k_1\Delta x]e^{\iota k_1 i\Delta x}\}\times \\
&\{[1-(\frac{1}{4}+\phi^2)(1-\cos k_2\Delta y) - \iota\phi\sin k_2\Delta y]e^{-\iota k_2 j\Delta y}\} \cdot e^{-\iota(k_1 vn\Delta t + k_2 wn\Delta t)} \\
&= \{[1-(\frac{1}{4}+\eta^2)(1-\cos k_1\Delta x) - \iota\eta\sin k_1\Delta x]\}\times \\
&\{[1-(\frac{1}{4}+\phi^2)(1-\cos k_2\Delta y) - \iota\phi\sin k_2\Delta y]\} \cdot \rho_{i,j}^{n} \\
&= (4.8)
\end{aligned}
$$

(II) The simplication of the right-hand side of (4.10) gives

$$
\begin{aligned}
\tan kx &= \frac{\epsilon\sin k\Delta x}{1-(\frac{1}{4}+\epsilon^2)(1-\cos k\Delta x)} \\
&= \frac{\epsilon[k\Delta x - \frac{(k\Delta x)^3}{3!} + \cdots]}{1-(\frac{1}{4}+\epsilon^2)(\frac{(k\Delta x)^2}{2!} - \frac{(k\Delta x)^4}{4!} + \cdots)} \\
&= \epsilon[k\Delta x - \frac{(k\Delta x)^3}{3!}][1 + \frac{1}{2}(\frac{1}{4}+\epsilon^2)(k\Delta x)^2 + \cdots] \\
&= \epsilon[k\Delta x + (\frac{\epsilon^2}{2} - \frac{1}{24})(k\Delta x)^3 + \cdots]
\end{aligned}
$$

Next, using the Taylor expansion approximation, we have

$$kx = \epsilon k\Delta x + \epsilon k\Delta x(\frac{\epsilon^2}{6} - \frac{1}{24})(k\Delta x)^2 + \epsilon O(k^5\Delta x^5)$$

This gives (4.11).

(III) Consider the case when $n = 0$ in (4.8). Substitute

$$\rho^o = e^{\iota\vec{k}\cdot\vec{r}} = \cos\vec{k}\cdot\vec{r} + \iota\sin\vec{k}\cdot\vec{r}$$

into (4.8) and let $\mathrm{Im}(\rho_{i,j}^{TD}) = 0$. This gives (4.12).

APPENDIX D

The "Projection" Of (3.18) Is Just (2.4)

If the "projection" of (3.18), the fully two–dimensional transport formula in uniform velocity field, onto the x–axis is defined as the sum of densities in (3.18) in the y direction for fixed x, then we have

$$\begin{aligned}
\rho_i^{TD} &= \text{"projection"} \quad \text{of} \quad \rho_{i,j}^{TD} \\
&= \frac{1}{64}\{(1+2\eta)^2[(1-2\phi)^2+2(3-4\phi^2)+(1+2\phi)^2]\rho_{i-1}^n \\
&\quad + 2(3-4\eta^2)[(1-2\phi)^2+2(3-4\phi^2)+(1+2\phi)^2]\rho_i^n \\
&\quad + (1-2\eta)^2[(1-2\phi)^2+2(3-4\phi^2)+(1+2\phi)^2]\rho_{i+1}^n \\
&= \frac{1}{8}\{[(1+2\eta)^2\rho_{i-1}^n + 2(3-4\eta^2)\rho_i^n + (1-2\eta)^2\rho_{i+1}^n] \\
&= \rho_i^n - \frac{\eta}{2}(\rho_{i+1}^n - \rho_{i-1}^n) + (\frac{1}{8}+\frac{\eta^2}{2})(\rho_{i+1}^n + 2\rho_i^n + \rho_{i-1}^n) \\
&= (2.4)
\end{aligned}$$

Similarly, there is a "projection" of (3.18) onto the y–axis.